Coupling of Chemical and Hydrodynamic Instabilities at the Electrochemical Dissolution of Metals

Kopplung von chemischen und hydrodynamischen Instabilitäten bei der elektrochemischen Auflösung von Metallen

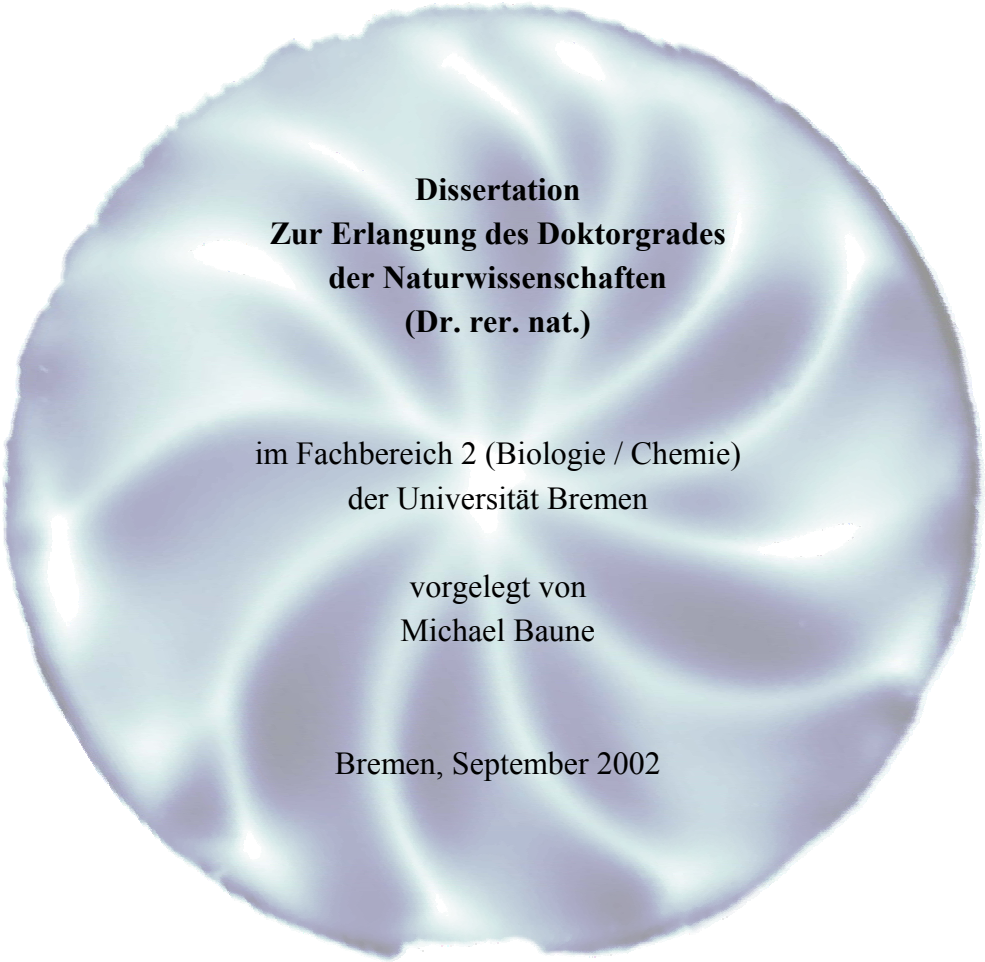

Dissertation
Zur Erlangung des Doktorgrades
der Naturwissenschaften
(Dr. rer. nat.)

im Fachbereich 2 (Biologie / Chemie)
der Universität Bremen

vorgelegt von
Michael Baune

Bremen, September 2002

1. Gutachter: Prof. Dr. Peter J. Plath, Universität Bremen, FB2
2. Gutachter: Prof. Dr. Nils I. Jaeger, Universität Bremen, FB2

Tag des öffentlichen Kolloquiums: 22.11.2002

The mind is amazing.
It starts to work the minute you're born and never stops
until you try to juggle.

Contents

Abstract

During galvanostatically controlled anodic dissolution of stainless steel in highly concentrated iron(III) chloride solution (3.5 M), etching patterns are formed in the surface of the rotating or non-rotating working electrode. Said pattern formations are the result of coupling between the hydrodynamics of the system and a strong dissolution process.
This dissertation examines experimental results of metal removal with regard to the electrochemical dissolution and hydrodynamic processes operating.
It was necessary to develop an applicative experimental setup which enables detailed galvanostatic/dynamic and potentiostatic/dynamic electrochemical measurements. In addition to thermostatic control of the reaction vessel, a videographic device was also required to enable observation of hydrodynamic pattern formation in and beneath the rotating disk electrode during an experiment. Due to the very strong light absorption of concentrated iron(III) chloride solution, a special lightning source was needed. Integrated into the experimental setup, it provided sufficient illumination of the working electrode and the solution beneath at low rotational speeds (0 - 50 rpm).
Using this setup, investigations of the dynamics of steel electrode dissolution at low as well as high rotational speeds were carried out.
The conditions for genesis of chemically induced hydrodynamic convection flow at resting and slowly rotating disk electrodes were studied. On the basis of these studies, the convection flow patterns beneath the electrode could be directly correlated with the etched patterns in the surfaces of the corresponding electrodes. Moreover, observed potential oscillations at slowly rotating disk electrodes under galvanostatic control could also be correlated with the etched patterns.
It was not possible to capture images during experiments at high rotational speeds (1000 - 6000 rpm) on account of the very fast movements in the solution as well as the strong light absorption of concentrated iron(III) chloride solution. However, the hydrodynamic flow emerges as an etched spiral pattern in the electrode surface, thus enabling detailed investigation of the structures after each experiment. These spiral-like patterns follow a logarithmic rule and feature an invariant curvature, even under different experimental conditions (such as a region of rotational speed, current density and temperature). This invariant behaviour of the spiral pattern formation in respect of external parameters can be explained physically, and a fixed ratio of tangential to radial flow of $1/\sqrt{2}$ was found for the curvature of the spirals generated.

Besides the formation of a topographically structured surface, the system exhibits galvanostatic potential oscillations. The interaction between the generated patterns and the galvanostatic potential oscillations was investigated. In addition to classical electrochemical oscillations, a new type of oscillation was detected. These superimposed oscillations could be correlated directly with the circular height profile of the topographically structured surface. It could be shown that this new type of oscillation is caused by the interaction between hydrodynamic vortex patterns in the boundary layer, on the one hand, and the electrochemical dissolution process, on the other hand, and that both these instabilities are coupled via the topographically structured surface of the electrode.
The experiments and theoretical interpretations shown in this work regarding the pattern formation at non-, slow and fast rotating disk electrodes under dissolving conditions provide a fundamental contribution to understanding the coupling between electrochemical processes and hydrodynamic flow at dissolving disk electrodes.

Kurzfassung

Bei der galvanostatisch kontrollierten anodischen Auflösung von Edelstahl in hoch konzentrierter Eisen(III)-Chlorid Lösung (3,5 M) kommt es zur Ausbildung von Ätzmustern in der Oberfläche ruhender oder rotierender Arbeitselektroden. Hierbei handelt es sich um eine hydrodynamische Strukturbildung, die mit dem starken Auflösungsprozess gekoppelt ist.
Im Rahmen dieser Arbeit wurden die experimentellen Ergebnisse des elektrochemischen Abtrags an der rotierenden Scheibenelektrode im Hinblick auf die Kopplung der elektrochemischen Auflösung und der hydrodynamischen Prozesse untersucht.
Hierzu war es erforderlich einen geeigneten experimentellen Aufbau zu entwickeln, der es ermöglicht, detaillierte galvanostatische/dynamische und potentiostatische/dynamische elektrochemische Messungen durchzuführen. Ein weiterer Anspruch an den Versuchsaufbau bestand, neben der Thermostatisierbarkeit darin, die hydrodynamische Strukturbildung in und vor der rotierenden Elektrode während eines laufenden Versuches videographisch zu verfolgen. Die sehr starke Lichtabsorption der konzentrierten Eisen(III)-Chlorid Lösung erforderte die Konstruktion einer speziellen Beleuchtungseinheit, die in den Versuchsaufbau integriert wurde und eine ausreichende Beleuchtung der Arbeitselektrode bei niedrigen Rotationsgeschwindigkeiten (0 - 50 rpm) gewährleistet.
Mit Hilfe dieses experimentellen Aufbaus wurden Untersuchungen der Dynamik des Auflösungsverhaltens von Stahlelektroden, sowohl bei niedrigen, als auch bei hohen Rotationsgeschwindigkeiten durchgeführt.
Es wurden die Entstehungsbedingungen natürlicher Konvektionen durch chemische Induktion bei ruhender und bei langsam rotierender Elektrode untersucht. Hierdurch konnte gezeigt werden, dass die Konvektionsmuster unterhalb der Elektrode direkt den eingeätzten Mustern in der Elektrodenoberfläche zugeordnet werden können. Auch die beobachteten Potentialoszillationen an rotierenden Elektroden unter galvanostatischen Bedingungen konnten eindeutig mit den auftretenden Ätzmustern korreliert werden.
Bei Versuchsreihen mit hohen Rotationsgeschwindigkeiten (1000 - 6000 rpm) war es nicht möglich, die Hydrodynamik unterhalb der Elektrode videographisch zu verfolgen. Da sich die hydrodynamischen Strukturen jedoch als spiralförmige Ätzmuster auf der Elektrodenoberfläche manifestieren, war es möglich, diese Strukturen im Anschluss an die Versuche genau zu untersuchen. Es konnte gezeigt werden, dass die eingeätzten spiralförmigen Muster, unter sehr unterschiedlichen Versuchsbedingungen, eine invariante Krümmung aufweisen. Diese Invarianz der Spiralmuster gegenüber externer Parameter

(wie z.B. Rotationsgeschwindigkeit, Stromdichte und Temperatur) konnte physikalisch erklärt und ein festes Verhältnis von tangentialem zu radialem Fluß, bezüglich der Krümmung der Spiralen, von $1/\sqrt{2}$ bestimmt werden.

Neben der Ausbildung topographisch strukturierter Oberflächen zeigt dieses System auch galvanostatische Potentialoszillationen. Die Wechselwirkung zwischen den entstandenen Strukturen und den Potentialoszillationen wurden im Detail untersucht. Zusätzlich zu den klassischen elektrochemischen Oszillationen wurde eine neuartige überlagerte Oszillation gefunden. Diese überlagerte Oszillation konnte direkt mit dem kreisförmigen Höhenprofil der topographisch strukturierten Oberfläche korreliert werden. Es konnte gezeigt werden, dass diese neue Art von Oszillation durch die Wechselwirkung zwischen hydrodynamischen Wirbelmustern in der Grenzschicht unterhalb der Elektrode und dem elektrochemischen Auflösungsprozess hervorgerufen wird, und dass diese beiden Instabilitäten über die topographisch strukturierte Oberfläche der Elektrode gekoppelt sind.

Die in dieser Arbeit durchgeführten Experimente und theoretischen Betrachtungen zur Strukturbildung sowohl an ruhenden Elektroden als auch bei niedrigen und hohen Rotationsgeschwindigkeiten tragen wesentlich zum Verständnis der Kopplung zwischen elektrochemischen Prozessen und hydrodynamischen Flüssen an sich auflösenden Scheibenelektroden bei.

1 Introduction

1.1 Fundamentals

The rotating disk electrode is an important technical facility for electrochemical investigations of galvanic dissolution and galvanic deposition of different metals. However, etching and deposition patterns occur in such systems under certain specific conditions (Basset & Hudson [1990], Krischer [1999], Fette [1995]). The coupling between hydrodynamic flow and the dissolution process plays a decisive role for galvanic moulding in microsystem technology and for electrochemical metal finishing processes in general (Visser & Buhlert [1999], Sydow et al. [accepted]).

Well-elaborated theoretical papers were found concerning the stability of three-dimensional boundary layers; this theoretical work provided the basis for understanding pattern formation at the rotating disk system (e.g. Gregory et al. [1955] or Levich [1962]).

In 1969, Piontelli et al. [1969] studied pattern formation during electrochemical deposition of metals at fast rotating disk electrodes. However, they did not focus on the feedback between hydrodynamic and electrochemical instabilities.

Many experimental and theoretical works have been published since, but the majority focus exclusively on the pure hydrodynamic transitions at rotating disks (Kobayashi et al. [1980], Kohama [1984] and Balachandra et al. [1992]). Not only the transitions directly at the rotating disk were described, but also the flow field in the bulk solution above a rotating disk (Spohn et al. [1998]). Rogers et al. [1963] investigated the influence of small roughness elements at the disk surface on mass transport. They discovered the formation of logarithmic spiral vortex patterns resulting from such roughnesses. The formation of logarithmic spirals on an electrode surface was first described by Yee et al. [1990] in their work on electrodeposition of zinc at rotating disks. Logarithmic spirals could also have been found by Piontelli et al. [1969] in the figures of their experimental results. However, they did not notice this formation of logarithmic spirals explicitly, so a connection to the work of Gregory et al. [1955] could not be established.

Recent experimental work concentrates on vortex flow in the transition region between circular and spiral pattern formation, which are interpreted in terms of instabilities of the stationary boundary layer at the electrode (Schouveiler et al [1999]). These statements are supported by Leneweit et al. [1999], who studied the instability of very thin liquid films on rotating disks.

There are only few publications about pattern formation on dissolving metals at rotating disks, despite the fact that the etching of metals plays an important technical role, particularly with regard to spray-etching of steel and copper alloys with highly concentrated iron(III) chloride solution (Visser et al. [1984] and Junker [1994]). In this connection, the investigations were mainly technical in orientation and did not deal with the dynamic processes of this system.
Traditionally, experiments at the rotating disk electrode are carried out at high rotational speeds in order to reduce the problems of transport to the double layer with nearly similar conditions at the whole electrode surface.
However, none of the theoretical works include variation of the electrode surface, which is essential for understanding the experimental results of pattern formation at the rotating disk.
In the present work, investigations were carried out at non-, slow and fast rotating and dissolving disk electrodes in order to understand the interaction between the hydrodynamics, pattern formation and the electrochemical dissolution of non-passivating metals, on the basis of stainless steel in highly concentrated iron(III) chloride solution.
These components were chosen on account of their common importance. Stainless steel, especially chromium nickel alloy (DIN 1.4301), is a material used very often in industrial applications and for private uses. During manufacture of metal products, highly concentrated iron(III) chloride solution (3.5 M) is deployed to burr edges, for example. It is also an important substance for etching printed circuit boards.
Investigations were therefore focused on the latter system. The problem of pattern formation in production processes can be abstracted in some respects to a rotating and dissolving disk electrode. Slow motions of workpieces can be represented by a slowly rotating disk, whereas a fast flow of solution along a workpiece can be simulated by fast rotating working electrodes. Additionally, galvanostatic controlled current can be applied to the system.
All experiments presented in this dissertation were carried out at a rotating disk electrode in a three-electrode setup under potentiostatic or galvanostatic control. The theoretical background for the single components and a description of the complete experimental setup are provided in detail in the sections that follow.

1.2 Theoretical Background

1.2.1 The Rotating Disk Electrode

In general, the rotating disk electrode is used to obtain exact experimental results pertaining to pure electrochemical processes at the electrode by controlling the influence of the diffusion boundary layer. Classical electrochemistry postulates a diffusion current flowing in orthogonal direction through the laminarly flowing boundary layer at the

rotating disk electrode. Due to the rotation of the disk, there is a constant vertical flow of solution from the bulk towards the electrode, as well as a horizontal flow from the centre to the edge. The flow conditions in the solution beneath the electrode were well described by Kármán [1921] and later by Levich [1962] and Newman [1973]. In these theoretical works, the flow towards the electrode is found to be independent of the radius (Fig. 1.1a), whereas the horizontal flow along the electrode is curved in the direction of rotation and follows spiral-like streamlines (Fig 1.1b).

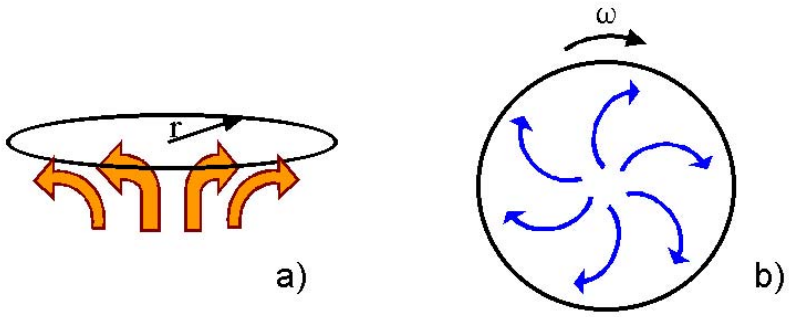

Fig. 1.1: Flow of solution towards the electrode (a) and along the surface (b)

In the present work, the main purpose of using the rotating disk electrode to examine coupling between electrochemical dissolution and hydrodynamic effects is to control a theoretically well-defined hydrodynamic flow along the working electrode.
However, as detailed in the sections 4 and 5, the flow and especially the idea of the fixed boundary layer at the electrode surface is not satisfactory if there is a coupling between the hydrodynamic flow and the dissolution of electrode material.

1.2.2 Three-Electrode Setup

Besides the defined control of the hydrodynamic flow at the working electrode, it is necessary to control and measure the potential and/or the current during an experiment. A typical three-electrode setup is used to separate the processes at the working electrode of interest from those at the counter electrode. This three-electrode setup was connected and controlled by a potentiostat/galvanostat (Fig. 1.2).

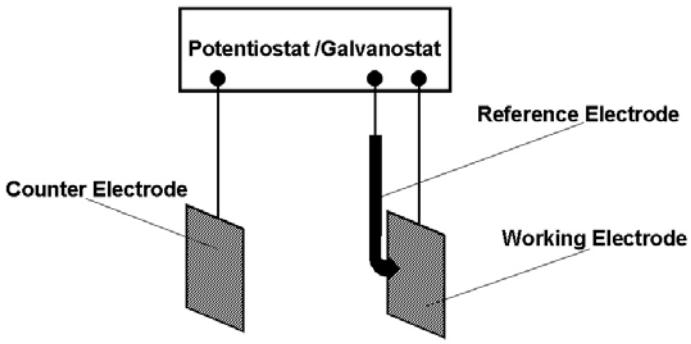

Fig. 1.2: Schematic view of a typical three-electrode setup

In order to set a defined potential at the working electrode, a comparison with a reference potential is essential. Said reference potential must be measured close to the working electrode (generally by means of a Luggin capillary) and its actual value compared with the ideal value of a potential generator in the potentiostat. If the actual differs from the ideal value, the potentiostat regulates the potential to the default by changing the current between working and counter electrode. Hence, the potential at the working electrode is always equal to the ideal value.
Galvanostatic measurements generally follow the same principle, except that instead of using the potential difference between working and reference electrode, a voltage drop at an internal resistance in the potentiostat circuit provides the reference value for regulation. In this case, the reference electrode only monitors the potential at the working electrode and has no influence on the regulation of the galvanostatic measurement (Hamann & Vielstich [1998]).
Potentiostatic and dynamic experiments were carried out to characterise the electrochemical system. Potential oscillations (identified by monitoring the potential at the working electrode) were found and analysed under galvanostatic conditions.

1.2.3 Electrochemical Oscillations

Electrochemical oscillations are a well-known phenomenon in electrochemical systems. A great variety of different types of oscillations, ranging from periodic, quasi-periodic, chaotic to intermittent behaviour are found to occur (Lee et al. [1985], Ma & Vitt [1999], Baune et al. [2000], Yang et al. [1998], Baier et al. [1999] or Wojtowicz [1973]). There is also considerable variation in the explanations given for the onset of electrochemical oscillations, as described in the following. The results of the present work can partly be seen in connection with classical electrochemical oscillations. However, a new type of oscillations was found and is detailed in the section 6.3.
As early as the beginning of the 19th century, Fechner [1828] reported electrochemical potential and current oscillations in a system comprising iron and silver in a HNO_3 - solution. A first detailed and systematical description of the periodic dissolution of chromium in hydrochloric acid has been given by Ostwald [1900, a & b)]. The basis for the first phenomenological model for electrochemical oscillations was mainly provided by Bonhoeffer [1948], Franck and FitzHugh [1961]. This electrochemical model is still of great importance for understanding current oscillations under potentiostatic control. It is based on a two-variable system - the solidity ratio of the passive layer on the electrode surface and the potential, which is calculated from the ideal potential set by the potentiostat, minus the Flade potential (Flade [1911]). Here, a pH dependency for the Flade potential is taken into consideration. The electrochemical basis for this model therefore involves a periodic shift of Flade potential caused by a change in the proton concentration in the diffusion layer at the electrode surface. Figure 1.3 shows a scheme for a typical current potential plot of a metal that can be passivated. Starting at the cathodic side, the

current rises with increasing potential due to the oxidation of the metal. With further increase in potential, the current reaches a limit because dissolution is now limited by transport. The shift (at the Flade potential) to the passive state is due to formation of an oxide layer that firmly adhering to the electrode surface according to the general reaction equation (Eq. 1.1):

$$Me + n\ H_2O \rightarrow MeO_n + 2n\ H^+ + 2n\ e^- \qquad (1.1)$$

In the passive state, the current remains at a very low residual current value, even though the potential rises. With the onset of oxygen evolution, the current increases again with increasing potential. This area of the current potential plot is called the transpassive region. For metals that cannot be passivated the system stays active until it reaches the transpassive state; no Flade potential or passive region can be observed.

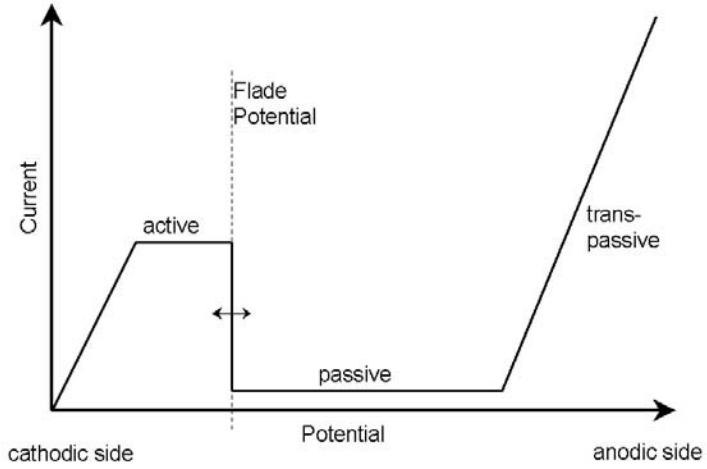

Fig 1.3: Schematic representation of a typical current potential plot for metals which can be passivated

When the state is in the active state, the proton concentration decreases in the diffusion layer and the Flade potential shifts to the cathodic side (left, Fig. 1.3). At the same time, the ratio of active to passive area at the surface decreases as well, and the current falls. In response, a lower dissolution rate occurs and migration of protons towards the electrode increases - the Flade potential shifts to the anodic side (right, Fig. 1.3) and the active passive cycle starts again.

Although this phenomenological model cannot describe dynamic behaviour more complex than simple periodic oscillations, it is taken as the basis for many new, modified models (Pearlstein & Johnson [1989], Wang et al. [1990], Otterstedt [1997] or Bîrzu [2001]).

For galvanostatic potential oscillations, other models and explanations need to be considered (Fette [1995], Li et al. [1990, 1993]).

Li et al. [1990, 1993] investigated, experimentally as well as theoretically, a system comprising iron in concentrated sodium-chloride solution. The potential oscillations observed have been attributed to the formation of an unstable porous salt layer of iron(II) chloride at

the metal, as opposed to the formation of a very dense oxide layer. The increasing thickness of the salt layer leads to rising resistance beneath the electrode and therefore to an increase in potential. In addition, some iron(II) is oxidised to iron(III); embedded in the salt layer and with a higher solubility than iron(II), the thickness of the layer again decreases. Due to this increase and decrease in salt layer thickness, an oscillation of potential can be observed.
Another explanation can be derived from the galvanostatic operating mode. If the current-potential curve shows a region with negative slope, two or more potential values have to be attributed to the default current value. This bistable situation can also be a cause of potential oscillations (Hamann & Vielstich [1998]).
The electrochemical oscillations shown in the present work (see section 6.3) could be explained by both of the aforementioned hypotheses. On the one hand, the formation of a visible, unstable and very dense colloidal layer at the electrode surface was observed (see section 4.3), thus pointing in the direction of the explanation provided by Li et al. [1990, 1993]. On the other hand, the potentiodynamic scan (presented in section 6.3) shows a region with negative slope, an indication that the explanation of galvanostatic potential oscillations provided by Hamann & Vielstich [1998] may be correct. In view of the foregoing, a decision as to whether the one or the other explanation is correct for the pure electrochemical oscillations observed (described in section 6.3) could not be made. However, the main focus of attention in this work was on the new type of oscillations caused by the topographical structure of the slowly rotating disk electrode.

1.2.4 Processes at the Electrode

The investigations were focused on the dissolution of chromium-nickel steel (DIN 1.4301, Appendix 2) in highly concentrated iron(III) chloride solution (3.5 M, Appendix 2). This system was used because of the very high dissolution rate of the metal, even without an additional current applied to the system. However, it was not the aim of this work to clarify the reaction mechanism at the working electrode.
As an example, the following scheme shows a mechanism which was suggested by McCafferty & Hackerman [1972] for an acidic system containing chloride:

$$Fe + H_2O \rightarrow Fe{\bullet}H_2O_{ads} \quad (1.2)$$

$$Fe{\bullet}H_2O_{ads} + Cl^- \rightarrow FeCl^-_{ads} + H_2O \quad (1.3)$$

$$FeCl^-_{ads} + H^+ \rightarrow [FeCl^-{\bullet}H^+] \quad (1.4)$$

$$[FeCl^-{\bullet}H^+] + H^+ \rightarrow FeCl^+ + 2H^+ + 2e^- \quad (1.5)$$

In this particular mechanism, a water molecule is firstly adsorbed by an iron atom, without oxidation occurring (Eq. 1.2). The next two steps (Eq. 1.3 and 1.4) describe the formation of an iron-chloride anion/proton complex. The final step (Eq. 1.5) is the oxidation of iron and the desorption of an iron-chloride cation.

Many other mechanisms have been described in the literature (Bockris et al. [1961], Chin & Nobe [1972] or Kuo & Nobe [1978]). They can all be applied to particular scientific questions, but, as mentioned above, it is only the strong dissolution that is important when studying the dynamics of pattern formation, not the means or mechanism by which the dissolution takes place.
However, in addition to these mechanisms one should consider the comproportion of iron and iron(III) to iron(II):

$$Fe + 2Fe^{3+} \rightarrow 3Fe^{2+} \tag{1.6}$$

This could play a very important role in the case of dissolution without an external current, especially. As could be shown (see subsection 5.3.2), current density has no influence on spiral pattern formation and dissolution rate at high rotational speeds, because dissolution of material for this system is strongly limited by transport of dissolved material from the electrode into the bulk solution.

1.3 Motivation

There are many phenomena in industry as well as in nature that are caused by interference between hydrodynamic motion at a surface and a process that modifies the topographical structure of the same surface. The following examples will give a brief impression of this problem and the great variety in which it occurs.

- The flow of water or wind along a sand surface can lead to a ripple formation (Fig. 1.4), as can be seen on the beach or in the desert (Andersen et al. [2002]).

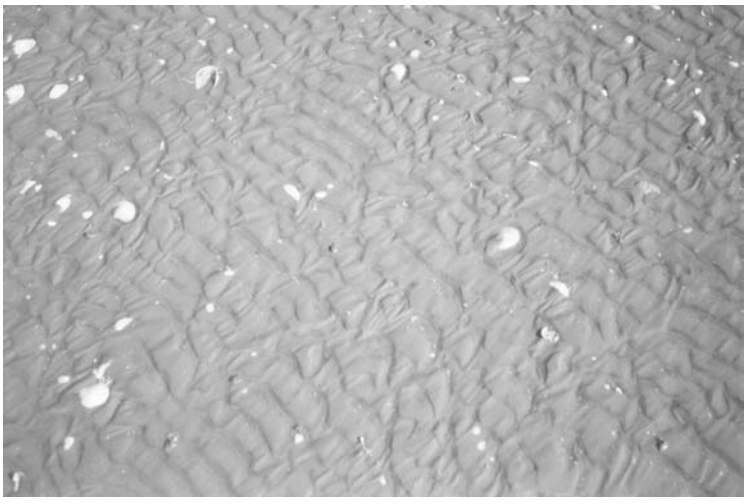

Fig.1.4: Ripples formed by the flow of water along a sand surface on the beach (Günther [2002])

- During the technical process of electro-polishing and -structuring, gas bubbles are formed at the surface. These bubbles create a hydrodynamic flow that results in macroscopic surface roughness (Sydow et al. [accepted], Visser & Buhlert [1996]).
- To cut material, a water jet is often used. However, due to the motion of the workpiece or the water jet, ripples are formed due to convective instability at the cut surface. (Friedrich [2000]).

This list could be continued to include the problem of pattern formation during electro-chemical machining for microstructuring (Kirchner et al. [2001], Ramasawmy & Blunt [2002]), or even for motion in the Earth's interior (Press & Siever [1995]).
The rotating disk was chosen because it enables precise control of a hydrodynamic flow by adjusting the rotational speed. The varying boundary conditions were obtained by means of strong dissolution of the metal disk electrode. Some of the aforementioned phenomena caused by the interaction between hydrodynamic flow and varying boundary conditions can be abstracted - in some respects - to the rotating and dissolving disk electrode.
The insights gained from this work are important for applications involving fast or slowly moving workpieces in corrosive media. Understanding how and under which conditions topographically structured surfaces are generated could help in avoiding unwanted pattern formation or in making specific use of these structures.

1.4 Aims of this Work

The aim of this work was to establish an experimental basis for better theoretical understanding of observed instabilities during dissolution of metals and alloys in convective systems. Experiments were carried out for the dissolution of stainless steel, which cannot be passivated, in a highly concentrated iron(III) chloride solution.
Interest was mainly focused on the influence of hydrodynamic flow on the structure of streamlines beneath the non- and slowly rotating disk electrode, on the one hand. This hydrodynamic flow can be caused by rotation of the disk as well as by a density gradient due to the dissolution process.
On the other hand, the experiments were aimed at investigating the influence of different parameters on the formation of logarithmic spiral-shaped patterns in the surface of fast rotating disk electrodes.
In both cases, the formation of vortices in the solution leads to topographical pattern formation in the electrode surface. Investigating these patterns can clarify the occurrence of hydrodynamic instabilities.
At a later stage, it was essential to investigate the time behaviour of observed galvanostatic potential oscillations with regard to the formation of convection patterns. The profiles of the surfaces had to be correlated with the time signals, and their interactions clarified.

The investigation of this coupling between the electrochemical etching process and the convective flow in the solution, leading to potential oscillations as well as macroscopic spatial etching patterns, shall form the basis for the theoretical understanding of such technically important systems.

2 Experimental Setup

In order to achieve the intended aims, it was necessary to provide the experimental requirements for:
- observation of the hydrodynamics in the solution
- thermostatic conditions
- regulation of the rotational speed and
- control potential and current.

The strong light absorption of 3.5 M iron(III) chloride solution posed a major problem for realising the videographic observation of the hydrodynamic flow beneath the electrode. Therefore, a UV-VIS spectrum of absorption of the solution was made in order to find the right wavelength with which to illuminate the electrode (Fig. 2.1).

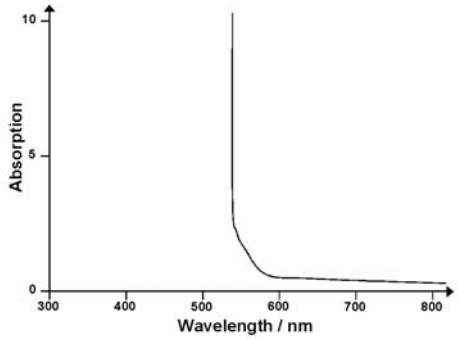

Fig. 2.1: UV-VIS spectrum of the 3.5 M iron(III) chloride solution showing a very low absorption above a wavelength of 605 nm

16 LEDs (Light Emitting Diodes) with a wavelength of 605 nm and an overall power rating of 1.68 W were then arranged in a circle. The light intensity was 9500 mCd for each LED. The circular arrangement (Fig. 2.2) was used as a dark-field illuminator, which enhances the contrast of surface features such as laser embossed or engraved marks, or surface defects.

This lightning source was embedded in an inert material (two-component epoxy resin, M9026, V. Höveling) and placed directly into the solution beneath the electrode at a distance of 2 cm (Fig. 2.3). Installing this special lightning source enabled sufficient light intensity for monitoring the hydrodynamics beneath the electrode. The low power of this construction also prevents the solution from unnecessary heating.

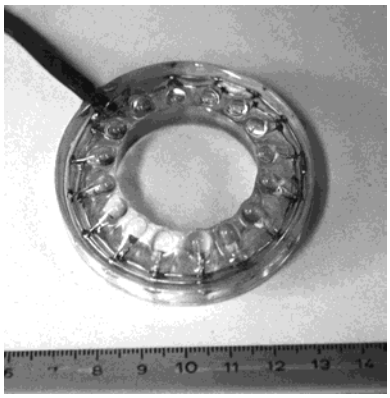

Fig. 2.2: Special lightning source with 16 LED's

An optical glass was integrated into the reaction vessel in order to avoid distortion while monitoring the processes at the working electrode and in the solution by means of the CCD camera (Fig. 2.3).
The reaction vessel consisted of a glass cylinder, 14 cm in diameter and enclosed in a heating/cooling jacket (Fig. 2.3) that enabled the temperature to be controlled with an external thermostat (LAUDA UB40). By designing the experimental setup in this way, it was possible to maintain the temperature in the reaction vessel at levels between 15 and 50°C.

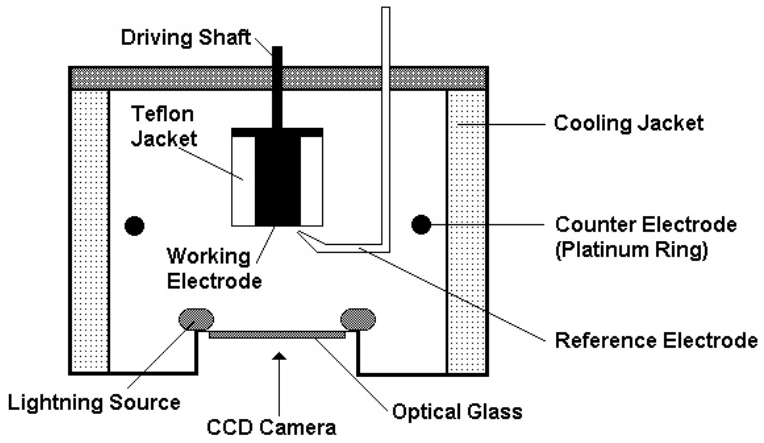

Fig. 2.3: Schematic cross-section of the reaction vessel with a three-electrode setup

The rotational speed of the working electrode could be set between 1 and 6000 rpm with an accuracy of 0.2% at 3000 rpm (according to the maker's specifications) by means of a rotation control unit (JAISSLE R.S. PI-REGLER).
A standard three-electrode setup connected to a JAISSLE potentiostat/galvanostat (IMP 83 PC-2) was used to control and measure both potential and current. The working electrodes (with a radius of 2.5 or 5.0 mm) consisted of chromium-nickel stainless steel (DIN 1.4301, Appendix 2) with a Teflon jacket for protecting the side walls (Fig. 2.4).

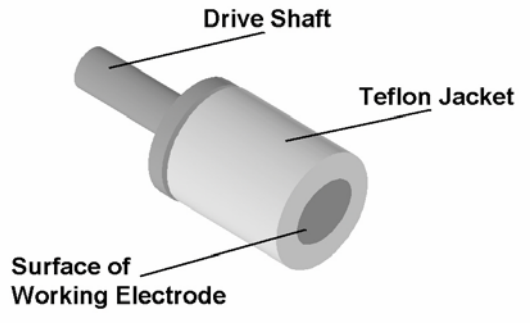

Fig. 2.4: Working electrode

A platinum wire with a diameter of 1 mm was used as the counter-electrode. It was placed circularly in the same plane as the working electrode, at a radial distance of 6 cm from the centre. The circular design of the counter electrode was chosen to guarantee radial distribution of current density.
To avoid hydrodynamic pattern formation being disturbed, the reference electrode (standard Ag/AgCl METTLER TOLEDO 363-S7/120) was placed via a Luggin capillary next to the edge of the working electrode (see also Fig. 6.1).
The overall setup is shown in Fig. 2.5.

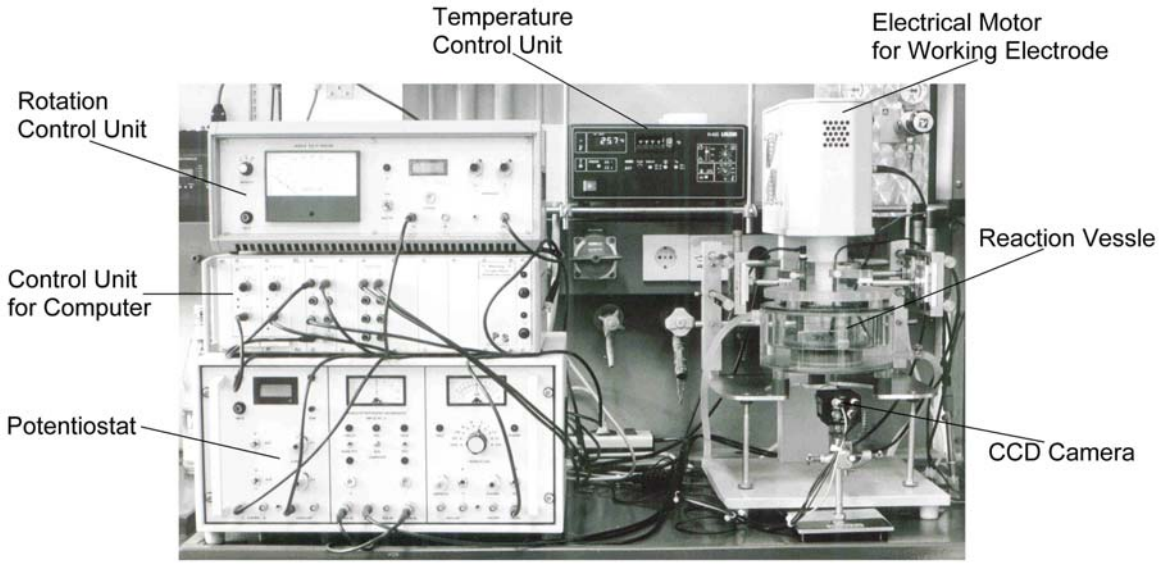

Fig. 2.5: The complete experimental setup

A personal computer (not shown in Fig. 2.5) was connected to the setup to control the potentiostat and rotational speed, to save potential and current data and to trigger the CCD camera and store the pictures.

3 Results

The onset of natural convection flow induced by a dissolution process for non-rotating as well as for slowly rotating disk electrodes is described in section 4, which is based on the article: "*Chemically Induced Hydrodynamic Pattern Formation: Slowly Rotating Disk Electrode under Dissolving Conditions and Genesis of Spatial Bifurcation*" (M. BAUNE and P. J. PLATH, In press: International Journal of Bifurcation and Chaos, Vol. 12, No. 10, October 2002)

This convection flow causes the formation of etched patterns in the surface of the electrodes. The shape of these formed patterns was observed to be dependent on rotational speed, and is explained in detail by a phenomenological model. For rotational speeds ranging between 0 and 50 rpm, the patterns in the surface were directly correlated with the convection flow beneath the electrode. Patterns generated at rotational speeds lower than 15 rpm are curved in the direction of rotation (Fig. 3.1, 10 rpm), because the processes which cause the formation of patterns are mainly influenced by the force of gravity. Processes at rotational speeds above 15 rpm, on the other hand, are mainly influenced by the centrifugal force, which results in topographical structures that are curved against the direction of rotation (Fig. 3.1, 20 rpm). A transition region at about 15 rpm was observed (Fig. 3.1, 15 rpm). This region indicates the point of balance between the two forces taking effect in opposite directions - the gravitational and the centrifugal force.

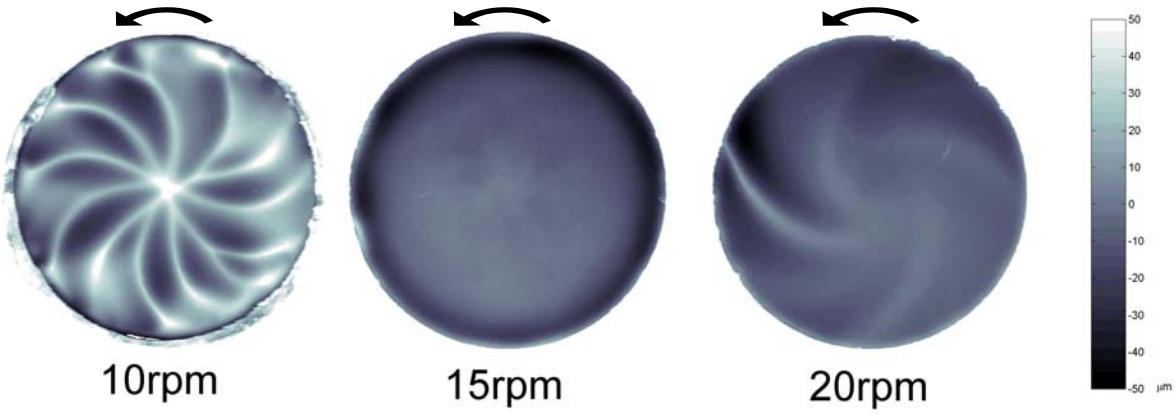

Fig. 3.1: Generated patterns with a change in curvature direction at different rotational speeds and a transitional region in between where no pattern is formed

The phenomenological model about convection vortices in the boundary layer was developed to explain the formation of the different topographically structured surfaces as well as the occurrence of spatial bifurcation in the patterns on the electrode.

In section 5, based on the article entitled "*Invariant Hydrodynamic Pattern Formation: Fast Rotating Disk Electrode Under Dissolving Conditions*" (M. BAUNE, V. BREUNIG-LYRITI and P. J. PLATH, Accepted for the International Journal of Bifurcation and Chaos), the behaviour of this system under conditions of fast rotating working electrodes (1000 – 6000 rpm) was investigated. Patterns with the shape of logarithmic spirals are generated at rotational speeds above 1000 rpm. When these spiral patterns were analysed, an invariant curvature of the structures was found. This invariant behaviour was identified for a broad range of external parameters, such as rotational speed, temperature, external current or the Teflon jacket enclosing the working electrode. Figure 3.2 shows the topography of a structured surface at 5000 rpm, with a superposed plot of two calculated spirals.

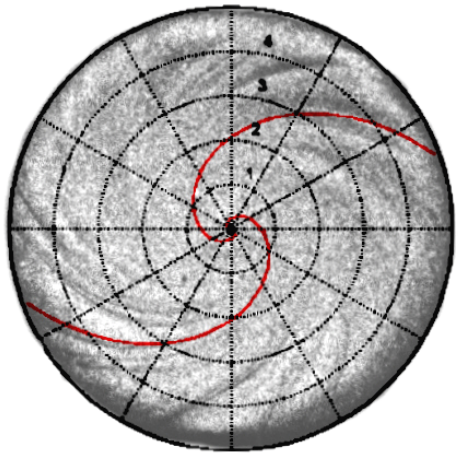

Fig. 3.2: Topography of a structured surface at 5000 rpm and two superposed calculated spirals

The shapes of the patterns were clearly determined as logarithmic spirals obeying the equation: $r = a \bullet e^{-b\phi}$. For all the patterns formed at high rotational speeds the value for *b* in this equation is about -0.71; this value results from the constant ratio between tangential and radial flow of $1/\sqrt{2}$ that was discovered. In contrast to classical explanations of pattern formation at rotating disk electrodes, the Coriolis force was taken into account and the invariance of the logarithmic spiral patterns could be explained by a physical description that takes into consideration the balance between tangential velocity, centrifugal and Coriolis force.

Beside the formation of etched patterns during the dissolution of stainless steel electrodes in highly concentrated iron(III) chloride solution, potential oscillations under galvanostatic conditions occur in this system and are presented in section 6, based on the article entitled "*Galvanostatic Potential Oscillations in a System with Electrochemically Induced Hydrodynamic Pattern Formation: Two Different Phenomena*" (M. BAUNE and P. J. PLATH, Submitted to PCCP).

A further aim of the experiments was to investigate the relationship between these electrochemical oscillations and pattern formation. Beside typical electrochemical oscillations (Fig. 3.3, blue curve), a new type of superimposed oscillations was found at low rotational speeds (Fig. 3.3, red curve).

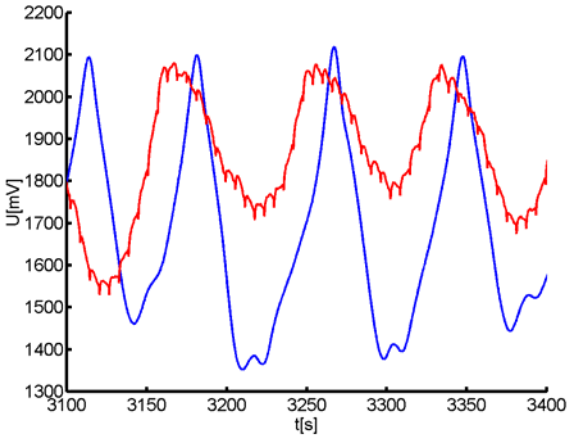

Fig. 3.3: Time series of pure electrochemical oscillation without rotation (blue curve) and electrochemical oscillation with a superimposed oscillation caused by the topography of the surface at a rotational speed of 10 rpm (red curve), both under galvanostatic conditions at 900 A/m^2

These superimposed oscillations are generated by the topographical patterns in the electrode and can be measured via the reference electrode, which simply monitors potential at the working electrode in the galvanostatic operational range. The periodic potential time signal shows a very high correlation with the height profile at a given radius on the corresponding electrode surface.

This new type of superimposed oscillation is caused by the interference of chemically induced hydrodynamic vortex patterns in the boundary layer beneath the rotating electrode with the oscillating electrochemical dissolution process. Both these instabilities are coupled via the topographical structuring of spiral patterns in the electrode surface.

4 Chemically Induced Hydrodynamic Pattern Formation: Slowly Rotating Disk Electrode under Dissolving Conditions and Genesis of Spatial Bifurcation*

Abstract

We investigated the system of a dissolving and slowly rotating steel disk electrode in an unstirred, highly concentrated iron(III) chloride solution (3.5 M). Visible convection vortices in the solution beneath the electrode were observed in the range of rotational speeds from 0 to 25 revolutions per minute (rpm). The convection vortices thus observed were correlated with etched patterns in the surface of the electrode. The curvature of these patterns was found to be dependent on rotational speed. At a certain value of the rotational speed (the transition region), the curvatures changed sign. A spatial bifurcation dependent on the radius was observed.

4.1 Introduction

The kinetic analysis of metal dissolution and of the dissolution process itself is a basic research field in engineering science that has been studied by many scientists during the past several decades ([Allen, 1986], [Visser, 1987], [Kuiken & Tijburg, 1999], [Visser & Buhlert, 1999]). The formation of hydrodynamic vortices in transition regimes of three-dimensional boundary layers on rotating disk electrodes has also been the subject of many investigations, because they reflect a variety of practical and academic interests ([Kármán, 1921], [Gregory *et al*., 1955], [Kohama, 1984], [Balakumar *et al*., 1991], [Leneweit *et al*., 1999], [Schouveiler *et al*., 1999]). However, the correlation between the convection flow at a rotating disk electrode and the electrochemical dissolution process is rarely found in the literature ([Fette & Plath, 1998], [Piontelli *et al*., 1969]). Hydrodynamic and electrochemical processes must be jointly analysed in order to obtain answers to the

* This chapter is based on the article: "*Chemically Induced Hydrodynamic Pattern Formation: Slowly Rotating Disk Electrode under Dissolving Conditions and Genesis of Spatial Bifurcation.*" (M. BAUNE and P. J. PLATH, In press: International Journal of Bifurcation and Chaos, Vol. **12**, No. 10, October 2002).

question as to the influence exerted by mass transport on the density and/or the viscosity of the boundary layer, or how an oscillating electrochemical process is coupled with a hydrodynamic system.
Fette & Plath [1998] reported on the galvanostatically controlled dissolution of steel in a concentrated $FeCl_3$ solution and the observation of potential oscillations without the formation of an active-passive transition at the electrode surface. These oscillations were found under galvanostatic conditions for various regions in the current density. They correlated the oscillations with travelling patterns of concentration regions beneath the disk electrode; a proposal for the mechanism is described in the PhD thesis of Fette [1995].
In the experiments described below, we investigated the patterns beneath and in the surface of the slowly rotating disk electrode, the formation of convection vortices in the solution beyond the electrode, and the coupling of hydrodynamic and electrochemical instabilities.

We observed different regions of pattern formation, depending on the rotational speed. The first observation was that there is a family of patterns in the region from non-rotating electrodes up to rotational speeds of about 15 rpm. A second phenomenon is found in the 20 rpm region. We characterised the transition regime between the different phenomena of these slowly rotating electrodes (0-25 rpm). Finally, we discuss the basic processes and the formation of patterns.

4.2 Experimental Details

The experimental setup is shown schematically in Fig. 4.1. It consists of a (Cr/Ni) stainless steel horizontal rotating disk electrode, with a radius of 2.5 or 5.0 mm, driven at a variable speed by an electric motor. The steel used is an ordinary Cr/Ni stainless steel with the DIN-number 1.4301. The rotation frequency is adjusted by an electronic controller with an accuracy of 0.2% at 3000 rpm (according to producer's specifications). A platinum ring is placed as counter electrode in the same horizontal position as the working electrode. These two electrodes are connected by an electrical conductor. The potential as well as the current is freely adjusted by the system. The optical glass at the bottom of the vessel and a specially developed lightning ring-source is also needed for recording the pattern formation using a CCD camera. The system is filled with 3.5 M $FeCl_3$ solution at a constant temperature (adjustable between 15 and 50 °C) and a kinematic viscosity of about $\nu \approx 6\ mm^2s^{-1}$ (at 25 °C).

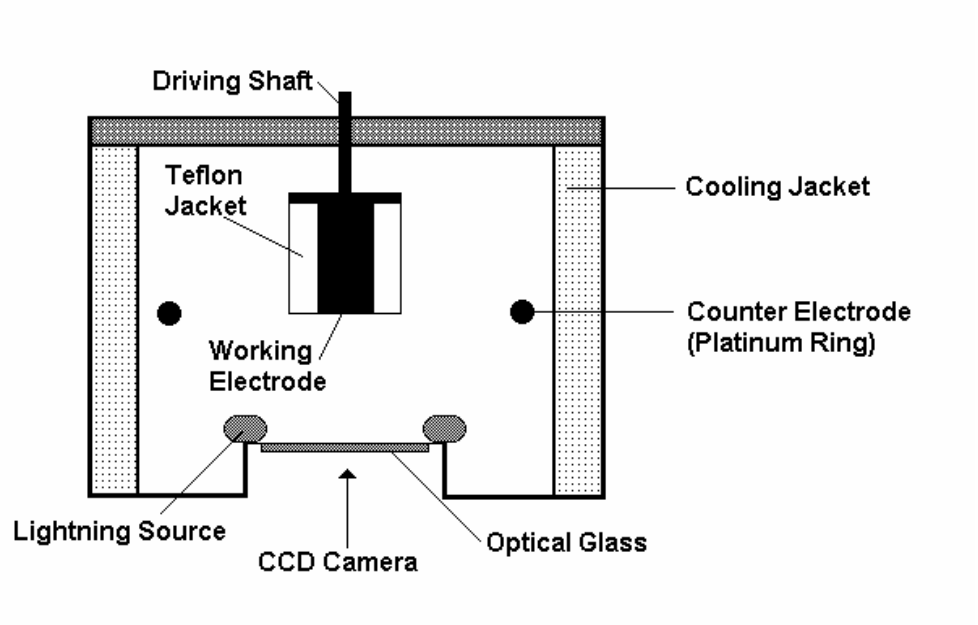

Fig. 4.1: Schematic cross-section of the reaction vessel

A laser-focus scanner (UBM microfocus) and additional digital image processing were used to visualise the patterns on the electrode surface after the etching process. Most of the pictures shown in this paper were generated by this method. The UBM microfocus gives a three-dimensional height profile of the electrode surface with a reticule resolution of 5 μm for the small (r = 2.5 mm) and 10 μm for the larger (r = 5.0 mm) electrodes.

The morphology of the metallic workpiece embedded in a Teflon jacket is shown in Fig. 4.2. The Teflon jacket consists of two different Teflon materials. The inner part, next to the metal, is soft Teflon and the outer part hard glassfibre Teflon. The whole Teflon jacket covers the metal in such a way that the working electrode has a plane and circular surface at the beginning of the experiment. The jacket also minimises the border effects during the etching process. The combination of soft and hard Teflon seals the space between the Teflon jacket and the metal of the electrode, thus preventing the $FeCl_3$ solution from penetrating the side wall of the electrode by capillary force.

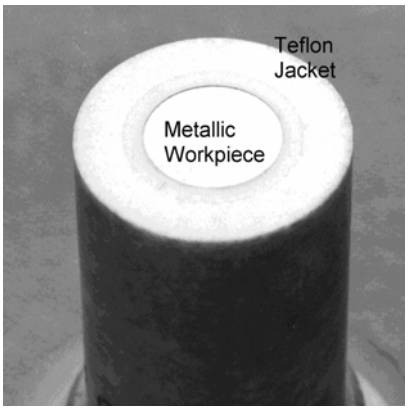

Fig. 4.2: The workpiece (electrode), for which the metallic part has a radius of 5 mm

4.3 Results

Our investigations were centred on two different processes. One process is the genesis and stability of convection vortices beneath the electrode due to dissolution process and the rotation of the electrode. We also analysed the formation of different patterns that were caused on the electrode surface by these convection vortices.
In the subsections that follow (4.3.1 and 4.3.2), we first show the different patterns formed in the regime with non- and slowly rotating electrodes. Subsection 4.3.3 then describes two other phenomena – firstly, the transition region, in which no patterns occur on the electrode surface, and, secondly, the observed spatial bifurcation of the patterns.
In subsection 4.3.4 we provide explanations for the basic processes underlying formation of the convection vortices and for the patterns on the electrode surface that are caused by the convection patterns.

4.3.1 Rotational speeds in the range 0 and 15 rpm

In the case of non- or slowly rotating disk electrodes, we observed various different patterns etched into the electrode surface. The constraints in all the experiments were the same: working temperature 25 °C, 3.5 M $FeCl_3$ solution, connection of the two electrodes using an electric conductor, electrode radius of 2.5 mm and a etching time of 60 minutes. Figure 4.3 shows the different patterns with rotational speeds of 0, 1, 2, 5 and 10 rpm (from left to right). The graphic representation of these surfaces was obtained by digital image processing of the Laser-focus (UBM microfocus) data scanned after the experiments.

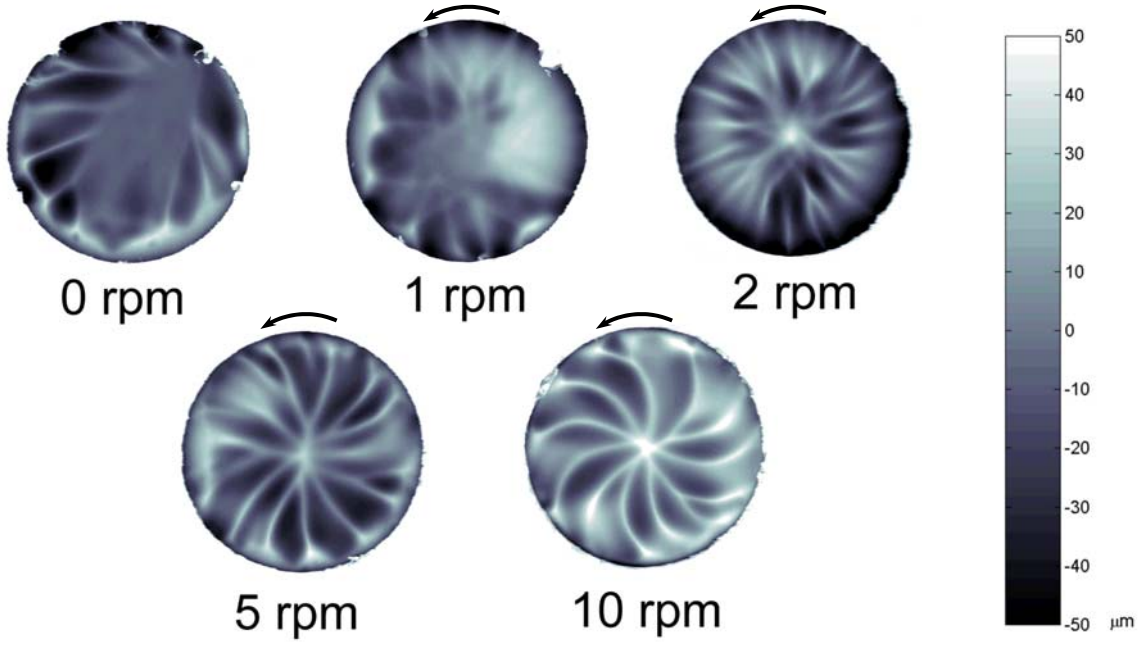

Fig. 4.3: Different (concave) patterns in the electrode surfaces (r = 2.5mm) after a etching time of 60 min. with different rotational speeds (from left to right: 0, 1, 2, 5 and 10 rpm); the direction of rotation is anti-clockwise

In these experiments we were able to show the increase in bending of the star-like and spiral patterns with increasing rotational speed. It was also shown that the patterns are bent in the direction of rotation. The number of 'spiral arms' decreases with increasing rotational speed.

In order to analyse the mathematical shape of the spirals for dependency of radius (r) on angle (φ), each of the digitised 'spiral-arms' were converted into polar-coordinates. By plotting these data as a φ - r plot, one should obtain, for example, a straight line for an archimedic spiral ($r = a*\varphi + b$). By analysing the single spirals in this way, it became clear that the etched patterns do not follow such a simple rule, but instead are rather like fingerprints. None of the structures have exactly the same shape. This means that the final result of the whole process is very sensitive to the initial and boundary conditions.

In almost all the experiments conducted, the φ - r plots feature a characteristic sharp bend in the curvature of the spirals at a certain radius (r = ca. 1.3 mm). This means we find a partly linear function that is not differentiable at r = ca. 1.3 mm. To make this proposition, we have to exclude the more or less linear structure of the experiments at 0 and 1 rpm. By way of example, a φ - r plot of a single digitised spiral is shown in Fig. 4.4.

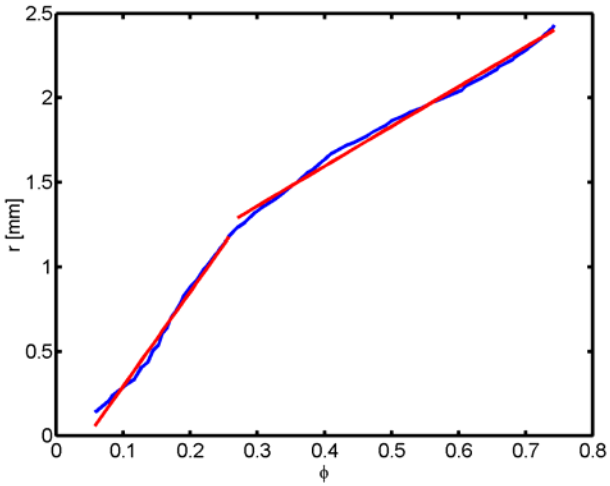

Fig. 4.4: φ-r-plot of a single digitised spiral with a change in curvature leading to a non-differentiable, partly linear function (r = a*φ + b); with a = 5.60 and b = -0.26 for left part and a = 2.36 and b = 0.65 for right part

4.3.2 Rotational speeds in the range 15 and 25 rpm

In these experiments we again found spiral-like patterns. However, in contrast to the experiments at up to 15 rpm, the bending of the patterns is in an anti-rotational direction, as shown in Fig. 4.5. The curvature in the anti-rotational direction (convex) is the shape that would be expected from the pure hydrodynamics without a dissolution process [Reed & Saric, 1989]. The number of 'spirals' in the range of 15 – 25 rpm is much less than in the above-mentioned experiments. The most important phenomenon is the change of curvature direction of the patterns at higher rotational speeds.

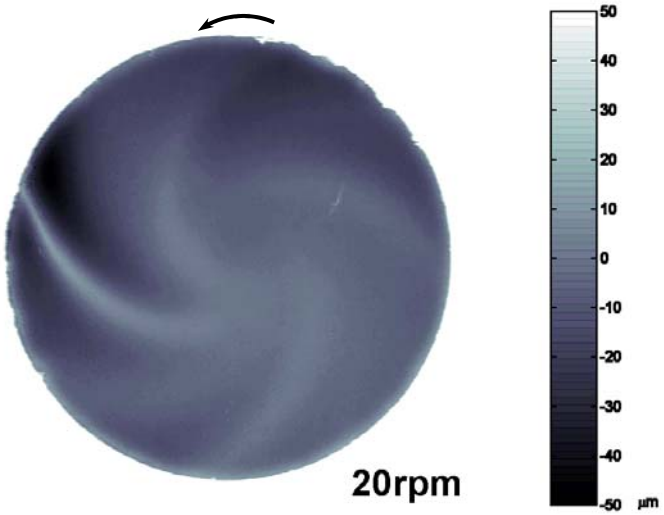

Fig. 4.5: Convex pattern in the electrode surface at rotational speed of 20 rpm; the direction of rotation is anti-clockwise

We thus defined the curvature direction as shown in the following sketch (Fig. 4.6). We called the curvature concave if it is bent in the direction of rotation (experiments at 0 to 15 rpm), and convex if the curvature is contrary to the direction of rotation (experiments at 15 to 25 rpm).

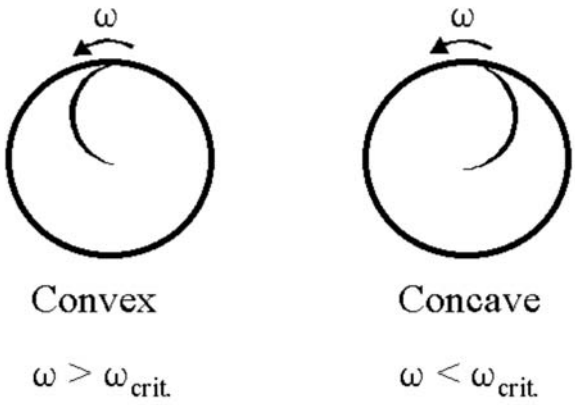

Fig. 4.6: Definition of curvature of structures at the electrode with respect to the rotation direction

4.3.3 Transition region at about 15 rpm and the spatial bifurcation

The resultant electrode surface at speeds around 15 rpm shows no structuring (Fig. 4.7). There is neither a star-like nor a spiral-like pattern etched on the metal surface. The explanation for this phenomenon is provided in the next section. Since we observed concave and then convex curvatures at increasing rotational speeds, we should also find a range of speeds at which no curvature in the patterns is observed. We identified such a critical region where we were unable to find any pattern at all on the electrode surface. The weak waviness that can also be obtained for this surface is caused by the border conditions of the surrounding Teflon jacket.

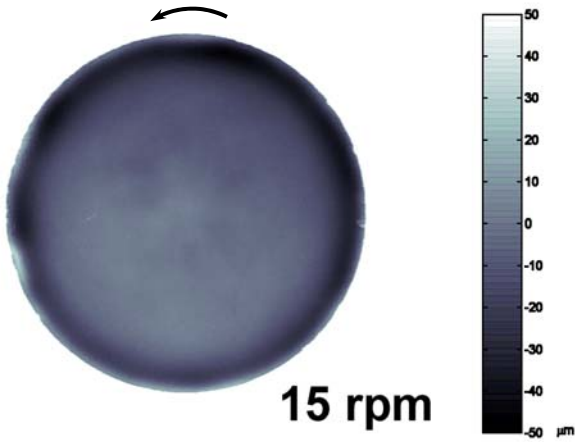

Fig. 4.7: The electrode surface at 15 rpm; rotation direction is anti-clockwise

Another phenomenon was discovered in the experiments conducted at rotational speeds around 10 rpm. In these cases, the spiral-like patterns exhibit splitting of the spirals. This phenomenon, which can be described as a spatial bifurcation, is illustrated in Fig. 4.8.

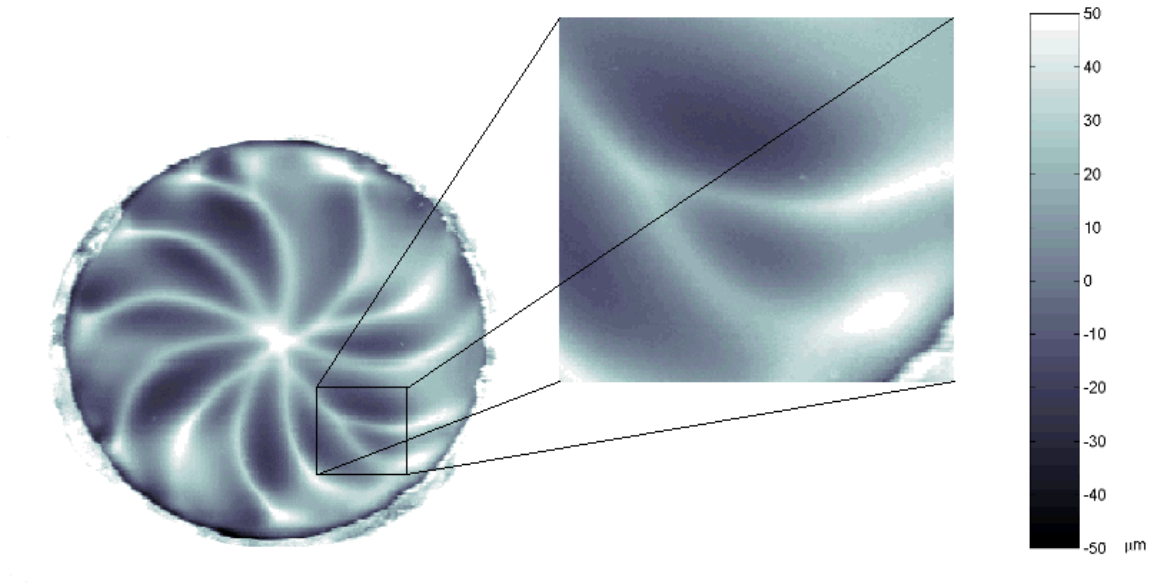

Fig. 4.8: Enlargement of the spatial bifurcation of the electrode etched for 60 min at a rotational speed of 10 rpm

4.3.4 Discussion of basic processes and pattern formation

During the etching process, we used a CCD camera to record the regions below the electrode in which the solution was of higher and lower density. Due to the fact that the darker parts of the solution sink in the gravity field, we assumed that these darker parts correspond to areas of higher density. Conversely, we can also assume that the lighter parts of the solution correspond to areas of lower density. These regions of different densities during the etching process are shown in Fig. 4.9 a. Compared with Fig. 4.9 b, one can see clearly that, in those parts of the electrode in which the solution has a lower density during the dissolution process, the steel electrode is etched more strongly than in those parts with higher density. This can be figured out by scanning the depth profile of the metal surface after the etching process.

Another factor is the convection flow that is initiated by higher-density solution sinking under gravitational force. By visualising the pattern formation in the solution and on the electrode surface during the entire dissolution process, we discovered that the electrode surface in the upstream region dissolves faster than in other areas. The ascending solution is always – in a first approximation – fresh bulk solution and therefore more reactive than

the used solution next to the electrode surface. As a result of the convection vortices generated in the solution, the used solution always moves to the regions beneath the electrode in which the solution is sinking. These effects provoke an intensification of the surface instability and lead to the generation of etched patterns in the surface.

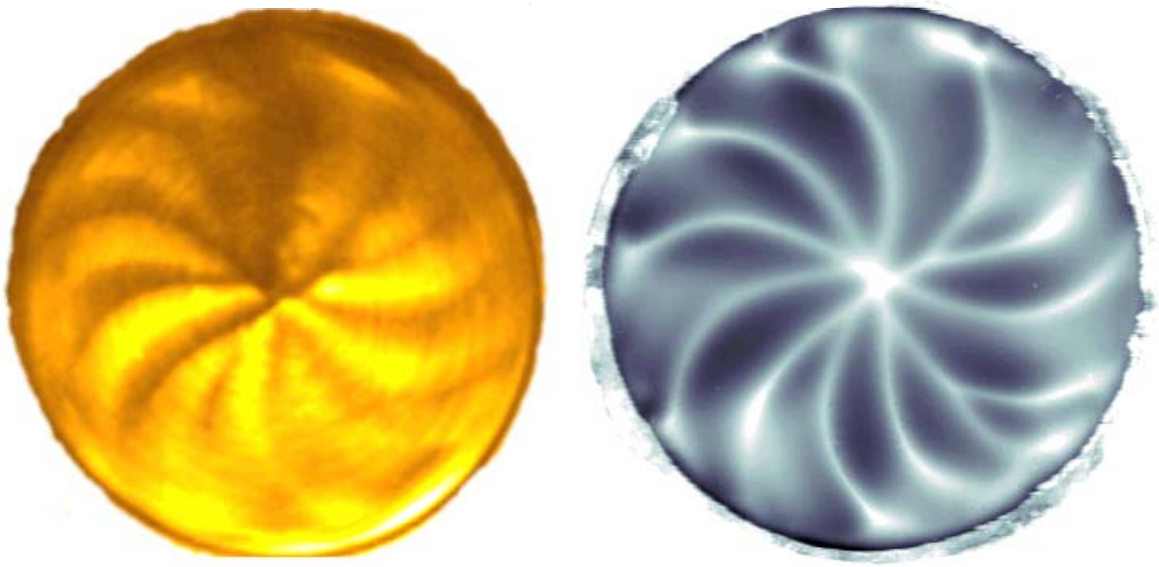

a) b)

Fig. 4.9: a) Vortices in the solution beneath the electrode surface (from CCD picture); b) Electrode surface after 60 min. etching (from UBM scan); a) and b) is the same electrode, with rotational speed of 10 rpm

These observations provide an explanation for why the electrode surface is not structured in the transition region around 15 rpm. However, we observed an unstable convection ring that breaks down either in a convex or concave convection vortex. It turned out that, in this regime of rotational speeds, none of the convection vortices beneath the electrode is stable enough to be fixed as a stable pattern in the surface.

The main direction of flow at low rotational speeds ($\omega < 15$ rpm) is from the edge of the electrode to the centre. This formation of a main flow results from the formation of a first colloidal salt layer on the electrode surface and its sinking down into the solution as a compact gel-like disk (Figs. 4.10 a and b). The driving force behind this phenomenon is the high density and coherence of the salt layer under the influence of the gravity field.

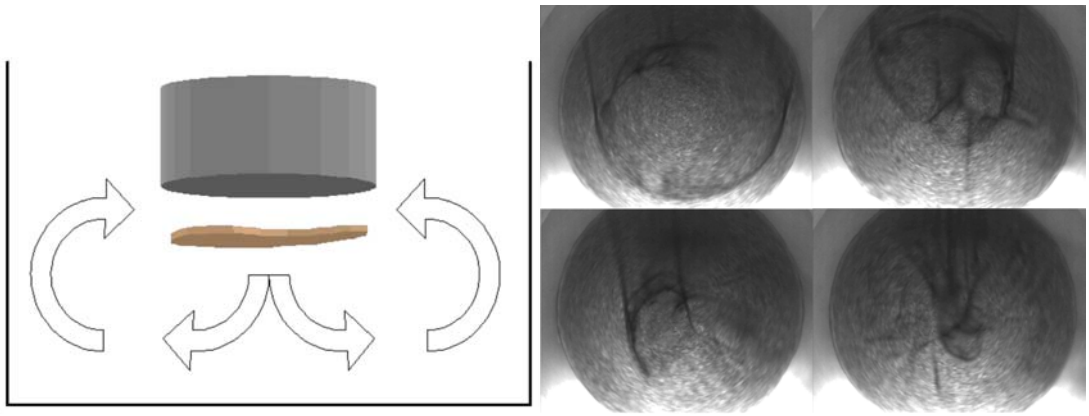

a) b)

Fig. 4.10: a) Schematic view of the onset of the main flow; b) In situ pictures showing the gel-like disk sinking

In the case of rotating disk electrodes, the sinking gel-like disk is stabilised by the rotation, which leads to a main, centrally symmetric convection flow.

In contrast to higher ($\omega > 15$ rpm) rotational speeds at which the main flow caused by the centrifugal movement of the denser solution is from the centre to the edge, in this case the salt layer generated is carried along by the flow induced by the rotation of the electrode itself.

Thus, in the case of slow ($\omega < 15$ rpm) rotational speeds, it is the force of gravity that exerts the predominant influence on centrifugal movement. At higher rotational speeds, the opposite is the case. These changes in the main direction of flow mean that the curvatures must have different directions at different rotational speeds, and that there must be a transition region.

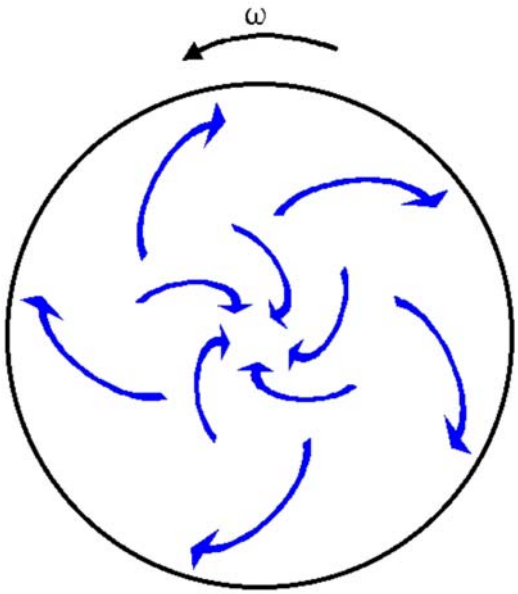

Fig. 4.11: Schematic view of the unstable convection vortices (blue arrows) beneath the electrode surface at a rotational speed of about 15 rpm

In the transition region, the lifetime of these unstable vortices is between about 3 and 20 seconds and leads to a continuous change in the curvature and flow direction of the convection patterns. A snapshot of these unstable convection vortices is shown schematically in Figure 4.11. As a result, one can see an almost unstructured surface (see Fig. 4.7) on the electrode after etching period (60min) has ended. This is caused by an averaging of the convection and etching processes.

If one assumes a critical size of the convection vortices, an explanation of the spatial bifurcation can be proposed. By over-stepping this critical size, one pair of convection vortices is separated by a newly generated, counter-rotating pair of vortices, as shown schematically in Fig. 4.12 a) and b). In Fig. 4.12 a) a basic approach for modelling the bifurcation of convection vortices is provided. The grey and black 'm-like' shapes represent parts of the structured surface of the electrode; the blue arrows represent the convection vortices in the solution beneath the electrode. The figure shows the splitting of two vortices and the genesis of a new pair of counter-rotating convection vortices. This results in a change of the electrode's surface.
In Fig. 4.12 b) the basic model can be compared with the bifurcation in a surface in an experiment conducted at a rotational speed of 10 rpm (shown in false colour representation).

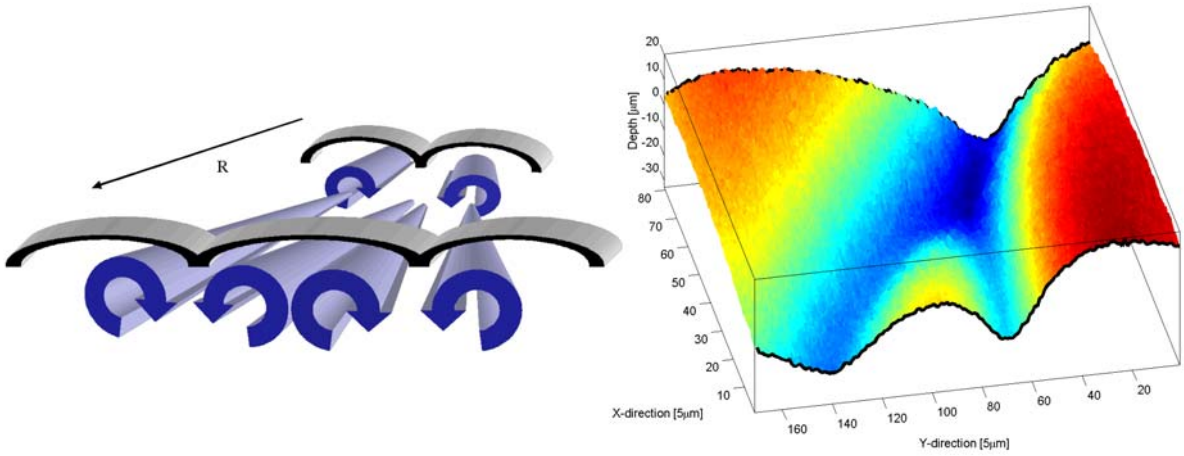

a) b)

Fig. 4.12: Comparison between a) a basic model of the vortex bifurcation and b) the experimental surface pattern shown in Fig. 4.8

4.4 Conclusion

Electrochemical dissolution of metals cannot be regarded without looking at the accompanying hydrodynamic processes. Convection patterns beneath the electrode surface appear even for slowly rotating electrodes, which lead to chemically induced convection patterns. A flow of fresh bulk solution in the upstream regions etches the surface strongly and creates slots, whereas the flow leaving the surface in the sinking regions contains much less reactive Fe^{3+} ions and cannot penetrate the surface as strongly as the fresh solution. Hence, the electrode is hardly etched and ridges between the valleys remain in the surface. For a hanging, non-rotating disk electrode the dissolution leads to a macroscopic pattern formation with arbitrary but self-stabilising hydrodynamic patterns, resulting in a non-symmetric shape of the etched pattern.

For very slow ($\omega < 15$ rpm) rotational speeds, the convection cells below the rotating electrode form almost periodic patterns, which result in concave, spiral-like patterns in the surface. The number of convection cells and hence the number of spirals in the surface diminishes with increasing rotational speed ω.

There exists a critical upper value of ω for which the concave patterns disappear and convex patterns occur ($\omega > 15$ rpm). These convex patterns also form spiral-like structures, but they do not start at the centre of the circular electrode. Their curvature changes with increasing rotational speed (rotation direction is anti-clockwise). Converting the single digitised spiral-arms into polar coordinates, the dependency of the curvature on the rotational speed can be expressed by a linear approximation ($r = a*\varphi + b$).

Without any rotation ($\omega = 0$ rpm) the radius of the patterns goes to infinity ($r \rightarrow \infty$).

In the range of rotational speeds between 1 and 10 rpm ($\omega = 1$ to 10 rpm), the radius of curvature changes from $r \approx \infty$ to $r \approx 2.5*\varphi + 1.0$ mm. This dependence of r on φ is only a first linear approximation and can be seen as an example for the range in which the spirals are formed.

In the range between 15 and 25 rpm ($\omega = 15$ to 25 rpm), we obtained in a first approximation the dependence: $r \approx -1.1*\varphi + 3.7$ mm. The basic purpose of these equations is to show the change in the sign of the factor a in the linear equation $r = a*\varphi + b$.

In the transition region, in which there is no structuring of the surface, we name the rotation a critical speed ($\omega = \omega_{crit.}$).

These curvatures are caused by the superposition of the centripetal ($\omega < \omega_{crit.}$) or centrifugal ($\omega > \omega_{crit.}$) movement of the dense solution (i.e. with higher concentration of dissolved material).

For a given radius ($r = 1.3$), a non-differentiable change in the curvature occurs, indicating the possibility of a spatial bifurcation in the spiral pattern. These bifurcations have been

observed experimentally. They are caused by convection cells that overstep a critical size, thus leading to a split into two counter-rotating convection vortices.
Finally, we can state that hydrodynamic structure formation at a dissolving, rotating disk electrode is strongly influenced by the chemical etching process, which creates radial (spiral) convection patterns and spatial bifurcations because of a mass-transport from the electrode into the solution.

4.5 Acknowledgement

We are very grateful to the 'Deutsche Forschungsgemeinschaft' for financial support (PL 99/8-1 and PL 99/8-2). We also thank Prof. A. Visser (Fertigungstechnik, Universität Bremen) for providing the microfocus scanner (UBM) and Prof. R. Friedrich and his workgroup (Institute for Theoretical Physics III, Universität Stuttgart) for inspiring discussions.

4.6 References

Allen, D.M. [1986] *The Principles and Practice of Photochemical Machining and Photoetching* (Adam Hilger, Bristol and Boston).

Balakumar, P. & Malik, M.R. [1990] "Traveling Disturbances in Rotating-Disk Flow," *Theoret. Comput. Fluid Dynamics* **2**, 125-137.

Balakumar, P., Malik, M.R. & Hall, P. [1991] "On the Receptivity and Nonparallel Stability of Traveling Disturbances in Rotating-Disk Flow" *Theoret. Comput. Fluid Dynamics* **3**, 125-140.

Fette, U. [1995] *Galvanostatische Potentialoszillationen und elektrochemisches Auflösungsverhalten von Edelstahl in Eisen(III)-chloridlösung, Ein neues oszillierendes System* (PhD Thesis, Universität Bremen) Chap. 9.10, pp. 97-102.

Fette, U. & Plath, P.J. [1998] "Galvanostatische Potentialoszillationen und anodisches Auflösungsverhalten von CrNi-Edelstahl in konzentrierter Fe(III)Cl_3-Lösung" *Zeitschr. für Phys. Chem.*, **205**, 143-165.

Gregory, N., Stuart, J.T. & Walker W.S. [1955] "On the Stability of Three-Dimentional Boundary Layers with Application to the Flow due to a Rotating Disk," *Mathem. and Phys. Sciences* **248**, 155-199.

Kármán, Th.v. [1921] "Über laminare und turbolente Reibung," *Zeitschrift für Angewandte Mathematik und Mechanik* **1**, 233-252.

Kohama, Y. [1984] "Study on Boundary Layer Transition of a Rotating Disk," *Acta Mechanica* **50**, 193-199.

Kuiken, H.K. & Tijburg, R.P. [1999] "Centrifugal Etching: A Promising New Tool to Achieve Deep Etching Results," *The Journal PCMI* **May**, 10-20.

Leneweit, G., Roesner, K.G. & Koehler, R. [1999] "Surface instabilities of thin liquid film flow on rotating disk," *Experiments in Fluids* **26**, 75-85.

Piontelli, R., Rivolta, B. & Razzini G.C. [1969] "Esempi tipici di effetti morfologici del moto relativo solido-liquido nei processi elettrochimici," *Elektrochim. Metal*. **IV**(3), 218-233.

Reed, H.L. & Saric, W.S. [1989] "Stability of Three-Dimensional Boundary Layers," *Ann. Rev. Fluid Mech.* **21**, 235-284.

Schouveiler, L., Le Gal, P., Chauve, M.P. & Takeda, Y. [1999] "Spiral and circular waves in the flow between a rotating and a stationary disk," *Experiments in Fluids* **26**, 179-187.

Visser, A. [1987] "Spray Etching of Stainless Steel - The Dependence of Stock Removal Rate on Alloying Elements and the Effects of High Sprayjet Pressures and High Etchant Temperatures," *The Journal PCMI* **30**, 8-15.

Visser A. & Buhlert M. [1999] "Theoretical and Practical Aspects of Fine Line Etching of Alloy 42," *The Journal PCMI* **May**, 21-26.

5 Invariant Hydrodynamic Pattern Formation: Fast Rotating Disk Electrode under Dissolution Conditions*

Abstract

During the dissolution of stainless steel in a highly concentrated iron(III) chloride (3.5 M) solution, patterns in the micrometer range can be observed on the surface of the rotating disk. These patterns are formed by convection vortices in the direction of hydrodynamic flow. At fast rotational speeds (2000 – 6000 rpm), the etched patterns are spiral in shape. By digitising the observed patterns, the mathematical equation for the spirals can be determined and a description obtained for their invariant logarithmic shape, with an aspect ratio of $1/\sqrt{2}$ for the radial and tangential velocity. A comparison with classical hydrodynamic equations for the rotating disk electrode and with the analysis of previous investigations of patterns formed on slowly rotating disk electrodes provides an explanation for chemically induced invariant hydrodynamic pattern formation.

5.1 Introduction

The phenomena of spiral vortices in the three-dimensional boundary layer beneath a rotating disk have been investigated by many scientists (Leneweit et al. [1999], Kobayashi et al. [1980], Gregory et al. [1955]). In addition, structure formation during electrochemical dissolution of metals and alloys in various liquid solutions (such as acids, bases and salt solutions) have been studied experimentally and theoretically (Bassett & Hudson [1990], Visser & Buhlert [1999], Kuiken & Tijburg [1999]). Knowledge about the kinetics of metal dissolution enables the dissolution process to be controlled. It is used to prevent the dissolution of metals (corrosion protection), on the one hand, and, on the other hand, to accelerate the dissolution process, since the latter is of prime interest for chemical and electrochemical machining in metal finishing production plants.

* This chapter is based on the article: "*Invariant Hydrodynamic Pattern Formation: Fast Rotating Disk Electrode under Dissolving Conditions*." (M. BAUNE, V. BREUNIG-LYRITI and P. J. PLATH, Accepted for: International Journal of Bifurcation and Chaos).

Not only is the prevention or acceleration of metal dissolution of great scientific and technological interest, but so, too, is the phenomenon of pattern formation during these processes as a result of coupling between electrochemical dissolution and hydrodynamic flow.
Based in most cases on the work of Levich [1962] on physico-chemical hydrodynamics, Riddiford [1966] and above all Piontelli et al. [1969] were the first, in the 1960s, to investigate electrochemical pattern formation on rotating disks during corrosion and deposition of metals.
Yee & Jorne [1990] initially compared observations of striated zinc depositions at a rotating disk electrode with the theory of Kármán [1921] and Cochran [1934]. They claimed that the experimentally observed logarithmic spirals followed the stream lines in the liquid layer beneath the rotating disk, and they predicted the characteristic angle $\alpha = 39.6°$ for the logarithmic spirals.
In our present work, we focused our investigation, by way of example, on pattern formation during the dissolution of stainless steel (DIN 1.4301) in a highly concentrated iron(III) chloride (3.5 M) solution on a rotating disk electrode at rotational speeds ranging from 1000 to 6000 rpm.

The results obtained from these fundamental experiments provide valuable information not only about metal finishing processes, but also with regard to astrophysical, geophysical and technological problems. This is because ship's propellors, turbo engines and motions in space, the atmosphere or the inner part of the Earth can be abstracted – in some respects – to the combination of chemical and hydrodynamic instabilities at the rotating disk under varying boundary conditions.

5.2 Experimental

A typical experimental setup for a rotating disk system was used with a specially developed lightning source. The chosen radii of the working electrode were 2.5 and 5.0 mm, and the side walls were protected by an embedding Teflon jacket. The solution used for the etching process was a 3.5 molar iron(III) chloride solution. With the help of a precision electrical motor, the rotation velocity of the working electrode was adjustable between 0 and 6000 revolutions per minute (rpm). The electrochemical reaction vessel, the topography of the working electrode, the experimental procedure and the technique for visualising the patterns in the electrode surface have been described in detail in a previous paper (Baune & Plath [2002]). In addition to the setup previously used, a typical three-electrode setup was installed in order to control and measure the potential (U) and the current (I).

5.3 Results

As an example, we focused our investigation on stainless steel electrodes at fast rotational speeds (e.g. 1000 – 6000 rpm) in a highly concentrated iron(III) chloride (3.5 M) solution. In this system, the stable and co-rotating boundary layer (with thickness δ) and a laminar flow in the bulk solution becomes unstable. Figure 5.1a schematically shows a view of the boundary layer (δ) and the convection flow at a rotating disk electrode in the bulk solution. Figure 5.1b illustrates the stream lines in the boundary layer as viewed from the electrode.

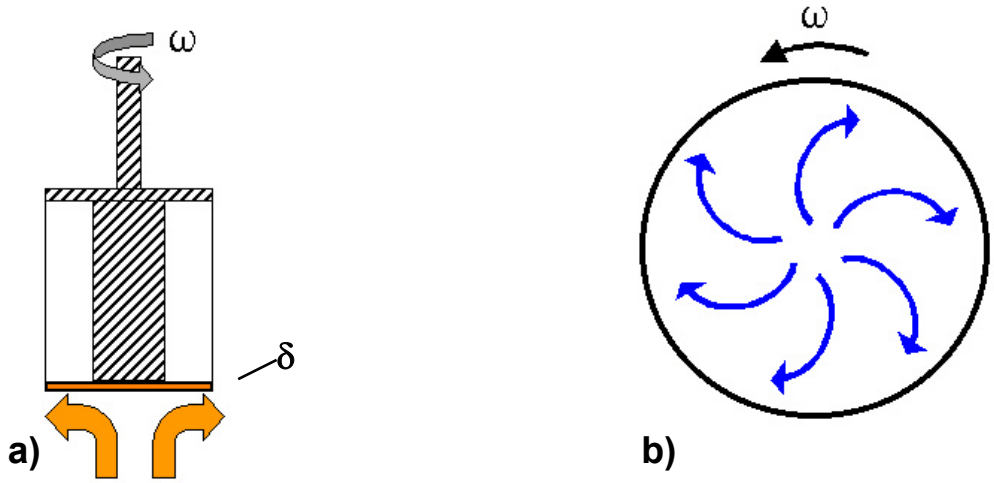

Fig. 5.1: a) Schematic view of the boundary layer (δ) and the convection flow in the bulk solution; b) Illustration of stream lines in the boundary layer, as viewed from the electrode

As a result of coupling between the hydrodynamics beneath the electrode and the strong dissolution process of the electrode, vortices are formed in the boundary layer and lead to pattern formation on the electrode surface. The structures on the surface of the metal that are caused by the dissolution process fix the vortices thus formed to the rotating electrode, which results in a growth of the structures in the metal and in a stabilisation of the vortices themselves.

5.3.1 Description of the patterns generated

The vortices in the boundary layer are turbulent rolls, which are curved as logarithmic spirals, following the stream lines of the convection caused by the rotation of the disk. These convection rolls in the boundary layer are fixed to the metal surface of the working electrode. The coupling of the strong dissolution process and the convection vortices (rolls)

leads to a pattern formation in the surface of the rotating disk that can be detected after the experiments when the electrode has been removed from the reaction vessel. Figures 5.2a and 5.2b show the surface of an electrode after total etching time of 5 min and a rotational speed of 2000 rpm. The patterns were detected using a laser-focus-scanner (UBM Messtechnik GmbH) with a resolution of 10 µm in the x and y axes, and 0.1 µm in the z-axis. Figure 5.2a shows the entire electrode surface (top view), whereas Fig. 5.2b only shows a quarter of the same electrode in a 3D perspective, which enables visualisation of the etching depth.

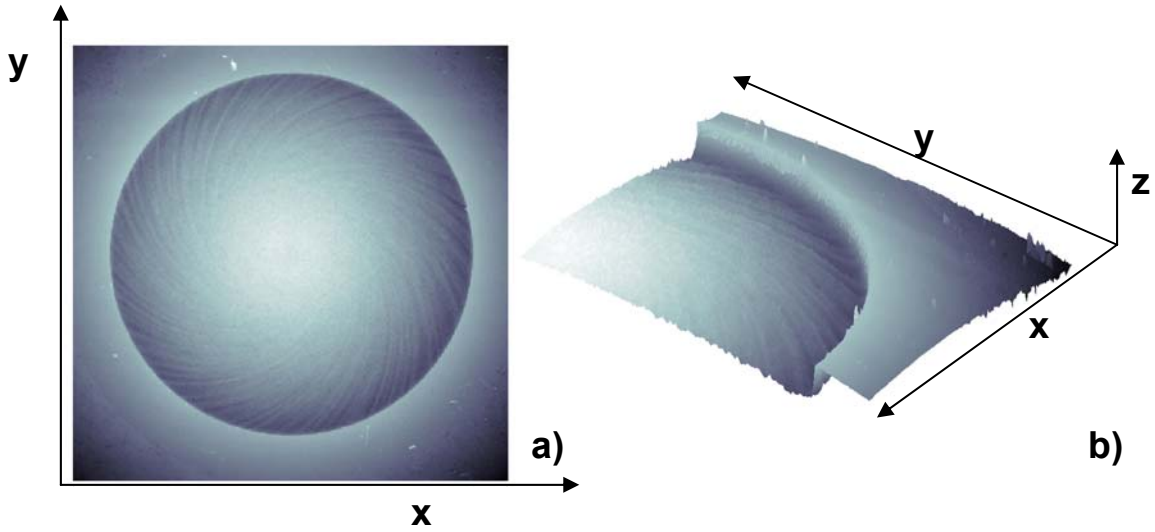

Fig. 5.2: a) Surface of an electrode with r = 5 mm after 5 min etching time at 2000 rpm and T= 25°C; b) 3D cross-section of the electrode shown in Fig. 5.2a

At the centre of the disk electrode, where a laminar flow can be assumed, one can find very fine etching patterns without any macroscopic global structure (Fig. 5.3, picture on left). These unstructured etching patterns are in the same order of magnitude as the grain boundary of the metal. However, the globally structured 'walls' and 'valleys' of the spirals formed also have these fine unstructured etching patterns. This can be seen in Fig. 5.3 (picture on right), which is a magnified view, obtained using a raster electron microscope (REM), into one of the 'valleys' of the spiral structure.

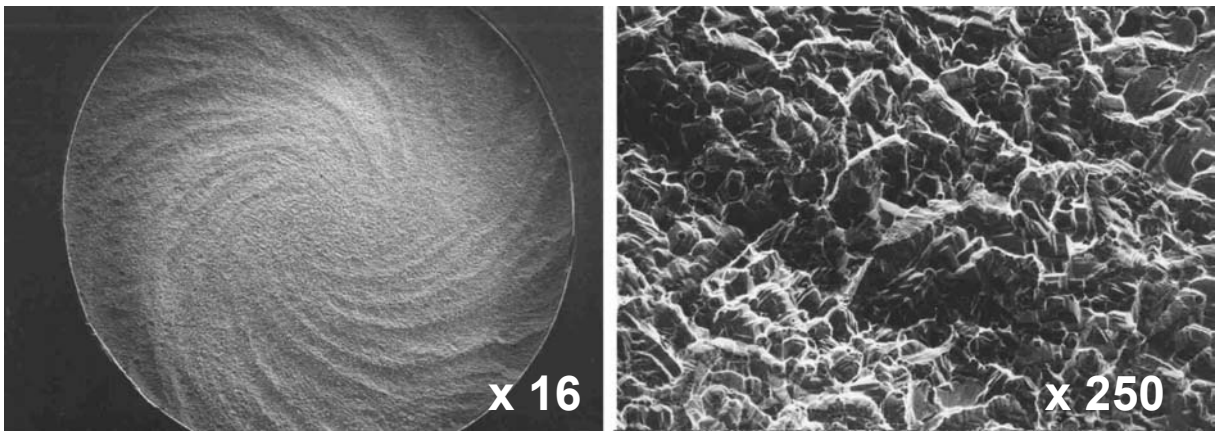

Fig. 5.3: REM zoom (x 250) into one of the 'valleys' of the spiral pattern (x 16) (5000 rpm; 50°C; 5 min)

This unstructured etched roughness in the electrode surface is important for showing that there is a coupling of hydrodynamic and electrochemical phenomena. The instability in the boundary layer beneath the electrode leads to a sequence of convection vortices that form a swirling flow. These vortices are fixed to the rough metal surface and follow the stream lines of rotation, resulting in etched spiral patterns on the electrode of the rotating disk with respect to the Coriolis force.

5.3.2 Factors affecting pattern formation

In the following section, based on experimental results, we discuss the influence of rotational speed, temperature, external current and the embedding Teflon jacket on pattern formation.

Dependency on rotational speed

A change in the rotational speed has an enormous effect on the formation of patterns on the electrode surface and on the amount of material dissolved. Fig. 5.4 shows electrodes with a radius of r = 5 mm and the development of patterns with increasing rotational speed. All of these experiments were carried out under the same conditions, in which current and power are freely adjusted by a conductive connection between the working and counter electrodes. The correlation between increasing etching depth and stronger formation of spiral patterns with increasing of rotational speed can be clearly identified. The dissolution rate rises from 2.0 mg/min at 1000 rpm, to 2.3 mg/min at 2000 rpm, to 3.5 mg/min at 5000 rpm. The onset of spiral pattern formation starts at rotational speeds of around 2000 rpm. The surface of the electrode dissolved at 1000 rpm shows no formation of spiral patterns. However, spiral patterns which are formed at 5000 rpm have a deeper profile and start closer to the centre than the structures formed at lower rotational speeds. At electrodes with a radius of r = 5 mm, the starting point (radius) of the spiral patterns shifts from r ≈ 2 mm (at 2000 rpm) to r ≈ 1 mm (at 5000 rpm).

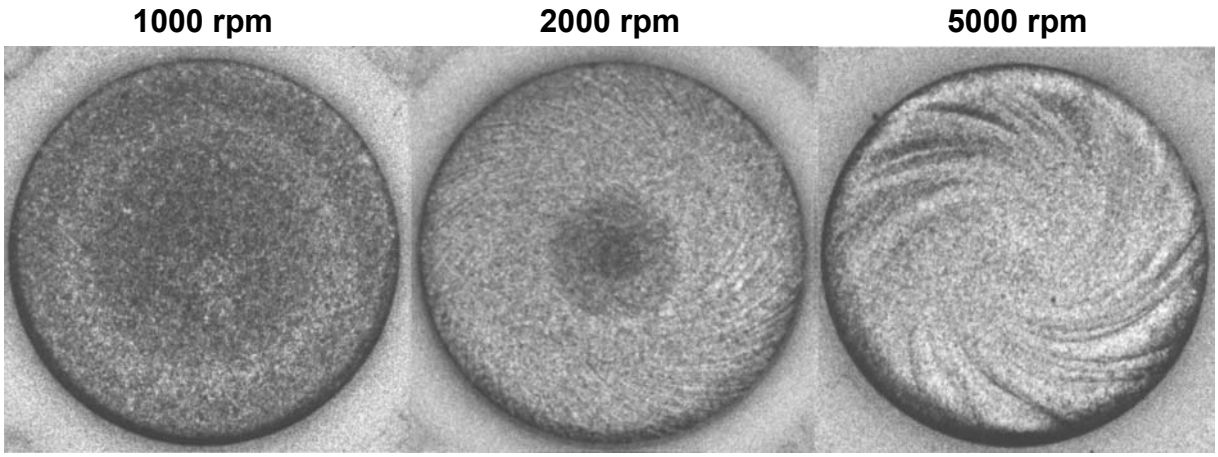

Fig. 5.4: Electrode surfaces after 50 min etching time and with increasing rotational speeds at T=25°C

It was found that different rotational speeds exert a strong influence on formation of patterns. Increasing rotational speed forces a shift and an intensification of convection vortices, leading to a higher dissolution rate, stronger pattern formation and the onset of spiral patterns closer to the centre.

Dependency on temperature

Due to the fact that an increase in temperature also means an increase in reaction rate and a decrease in viscosity (BASF Info Service [2001]), changes in pattern formation should be expected as temperature is increased. In accordance with the expected phenomena, these changes were also detected experimentally. Figure 5.5 contrasts electrodes after an experiment conducted at a temperature of 25°C (left) and 50°C (right). The radius of both electrodes is r = 5 mm, and the results were obtained at 5000 rpm.

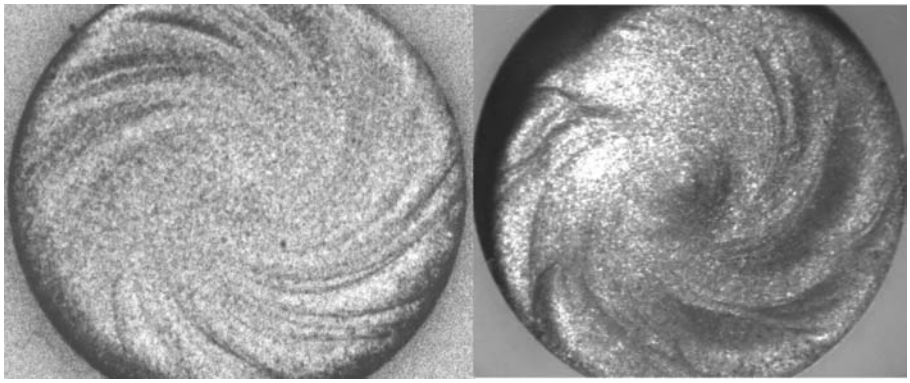

a **b**

Fig. 5.5: Surface of an electrode (r = 5 mm) after 50 min etching time at 5000 rpm;
a) T = 25°C and b) T = 50°C

This experimental result shows the influence of temperature on structure formation. The patterns formed are more strongly developed with higher temperatures, similar to the changes with increasing rotational speed. Here, too, the dissolution rate increases from 3.5 mg/min at 25°C to ca. 11 mg/min at 50°C.

In addition to the effects of temperature on pattern formation at high rotational speeds, an influence of temperature on the convection flow at slowly rotating disks could also be detected experimentally. As we reported previously (Baune & Plath [2002]), the natural convection flow at very slow rotational speeds, or even without rotation, can cause pattern formation on the electrode surface. In Figs. 5.6a and 5.6b, a significant change in pattern formation at a rotational speed of 10 rpm was discovered by changing the temperature from 25°C to 50°C. Increasing the temperature leads to a decrease in the viscosity of the solution. This means that the natural convection flow from the edge to the centre of the electrode becomes faster. The faster convection flow results in a straightening (Fig. 5.6b) of the curved patterns (Fig. 5.6a) generated at the same low rotational speed (10 rpm) and room temperature (25°C).

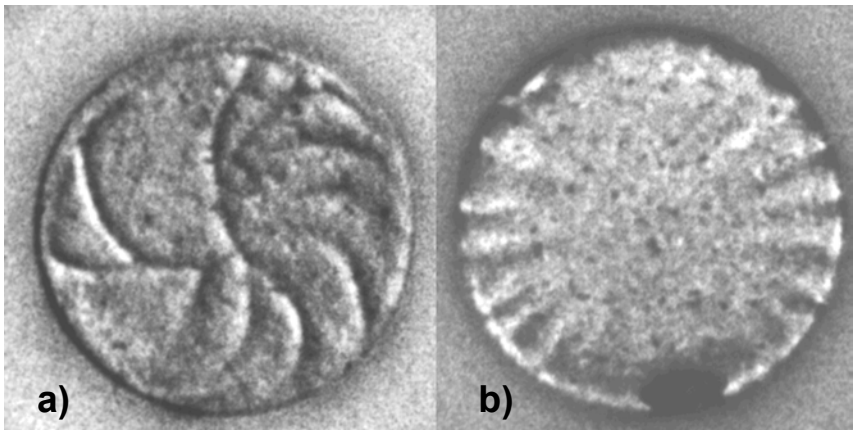

Fig. 5.6: Pattern mainly caused by natural convection flow at 10 rpm; a) T = 25°C and b) T = 50°C

In summarising the influence of temperature on pattern formation, it is important to point out the differences between fast and slow rotational speeds. On the one hand, the patterns which are formed at slow rotational speeds change their shape completely, given that temperature exerts substantial influence on the natural convection flow. On the other hand, increasing the temperature at fast rotational speeds has an effect on pattern formation similar to that caused by increases in rotational speed. Only the dissolution rate rises, and the patterns are profiled more strongly, but the curvature does not change.

Dependency on external current

As is well known from electrochemistry, the dissolution of material in a classical electrochemical cell is proportional to the amount of current (Fette [1995]).

$$m_{ox} = k \cdot I \cdot t \tag{5.1}$$

However, in this system – stainless steel in a highly concentrated iron(III) chloride solution – the dissolution caused by the very aggressive solution must be taken into consideration. In the following figures (Fig. 5.7a-c), pattern formation at 5000 rpm is shown under different conditions for the external current.

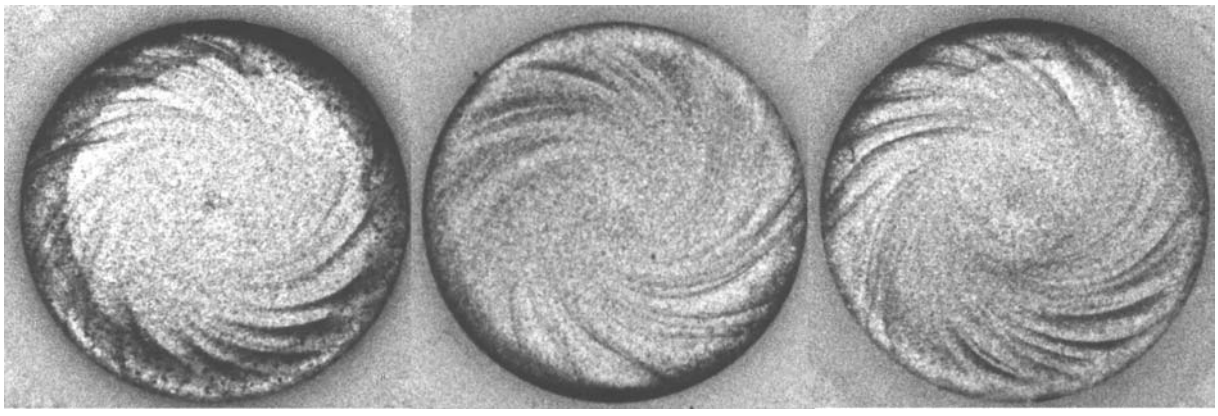

Fig. 5.7: Pattern formation at 5000 rpm and T=25°C: a) constant current of 3000 A/m^2; b) free corrosion potential with I = 0 A; c) I and U are freely adjusted by the system itself

Figure 5.7a shows a surface after an experiment conducted with a constant current of 3000 A/m^2 applied to the electrode. Figure 5.7b is an electrode at the free corrosion potential without any current flow at all. Fig. 5.7c is the result of an experiment in which both the potential as well as the current are freely adjusted by the system itself, via an electrical conductor connecting the working and the counter electrode. All experiments conducted under these different conditions resulted in almost identical phenomenological patterns and almost the same etching depth.
An estimation of the dissolved material (Fe^{2+} : Fe^{3+} = 1:1) at a fixed current of 3000 A/m^2 of about 3.4 mg/min is in the same order of magnitude compared to the dissolution rate of 3.5 mg/min at 5000 rpm caused by the aggressive iron(III) chloride solution.
This leads to the conclusion that pattern formation in this system is strongly limited by the transport of dissolved material, but not by the way it was dissolved. If there is no current, the dissolution is caused by the aggressive iron(III) chloride solution, but with a high external current the solution stays almost fresh even for long running experiments.

Embedding Teflon jacket

In this section, proof is provided that pattern formation is not dependent on or caused by the Teflon jacket embedding the metal workpiece. To this end, an experiment was carried out with a cylindrical metal electrode that had no protection for the side walls. The result is given in Fig. 5.8a, in comparison with the results previously shown (Fig. 5.8b).

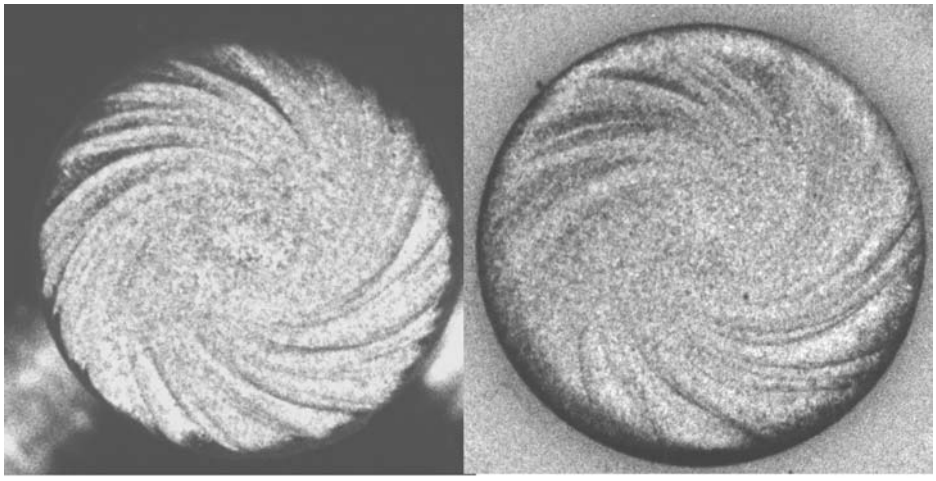

a **b**

Fig. 5.8: a) pattern formation at 5000 rpm without embedding Teflon jacket; b) pattern formation at 5000 rpm with embedding Teflon jacket; both at a temperature of T = 25°C

The rotational speed in both experiments was 5000 rpm. These experiments prove that the convection vortices which cause the patterning on the electrode surface are actually generated by the coupling of hydrodynamic and dissolution, but not by the effect of the embedding Teflon jacket.

5.4 Theoretical description of the spirals generated

It has been mentioned that spiral-shaped patterns are formed on the disk electrode at rotational speeds between 2000 and 6000 rpm. These spiral patterns are etched into the surface of the electrode and can be measured after the experiments. To study the curvature of these spirals in more detail, single spiral 'arms' were digitised (Fig. 5.9a) and plotted with polar coordinates (ϕ-r plot; Fig. 5.9b) in order to find the dependence of the radius (r) on the angle (ϕ). All the spirals generated at high rotational speeds are logarithmically shaped and can be described by the following equation (with: r = radius; ϕ = angle; a and b = const.):

$$r = a \cdot e^{-b\Phi} \tag{5.2}$$

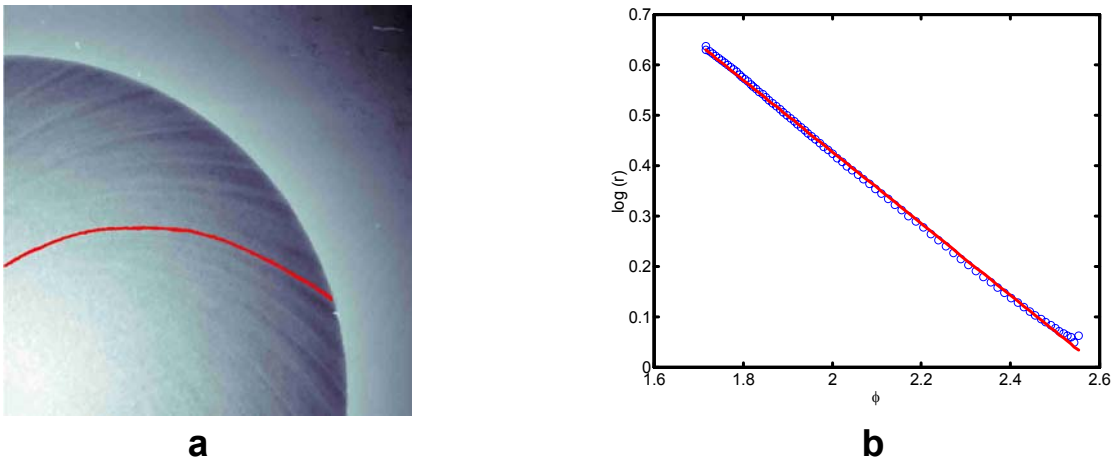

Fig. 5.9: a) Example of one digitised spiral arm of generated pattern at 6000 rpm and T = 25°C; b) ϕ-r plot of the digitised spiral arm; (blue: plot of the logarithmic values of r; red: fitted logarithmic values with a = 6.4 and b = – 0.71

Logarithmic spirals are characterised by the independence of the angle (α) on the radius (r) (see Fig. 5.10). The value of ***tan*** **α** is equal to the constant **b** of Eq. 5.2.

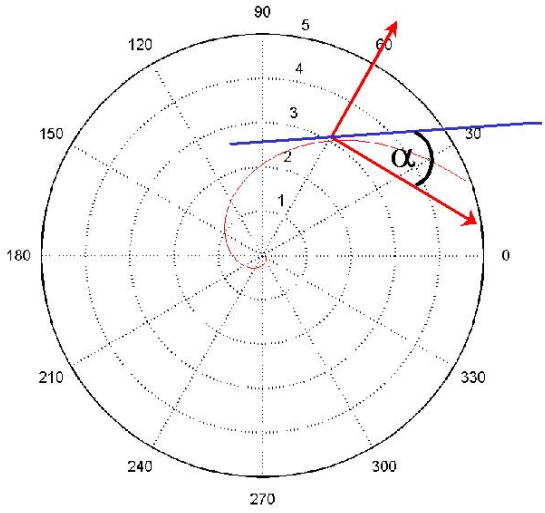

Fig. 5.10: Schematic view of the invariant angle α

In the case of experimentally generated, spirally shaped patterns on a stainless steel electrode in iron(III) chloride solution, an angle α of about 35° was determined. This value for α is not only independent on the radius (r), but also valid for quite different speeds. For all experiments conducted at rotational speeds between 2000 and 6000 rpm, a value for α in the range of 35° was observed. In addition, we measured the same angle for generated spiral patterns described in other publications (see Table 5.1) for completely different electrochemical processes on rotating disk electrodes.

Conditions	**Source**	**Measured angle (α)**
Steel dissolution in $FeCl_3$ solution (ω = 2000 rpm; T = 25°C, free potential)	Own experimental results	**36°**
Steel dissolution in $FeCl_3$ solution (ω = 6000 rpm; T = 25°C, free potential)	Own experimental results	**36°**
Steel dissolution in $FeCl_3$ solution (ω = 5000 rpm; T = 50°C, free potential)	Own experimental results	**35°**
Steel dissolution in $FeCl_3$ solution (ω = 5000 rpm; T = 25°C, I = 3000A/m^2)	Own experimental results	**34°**
Deposition of copper from alkaline cyanide solution	Rogers & Taylor [1975]	**35°**
Nickel plated from Watts solution	Rogers & Taylor [1963]	**35°**
Etched pattern (general description)	Levich [1962]	**34°**
Deposition of cadmium on copper	Piontelli et al. [1969]	**35°**

Table 5.1: Examples of graphically measured angles α in some of our own experiments, and of experimental results from other publications (accuracy of α is ± 0.5°)

This means that the spiral patterns generated electrochemically on rotating disks obey the same logarithmic rule and are invariant with respect to the radius, quite different rotational speeds and even different electrochemical systems.
Investigating the angle α of about 35° more carefully, it could be described as a combination of two orthogonal vectors, in the same plane of the disk, with a fixed ratio of $1/\sqrt{2}$ (Fig. 5.11).

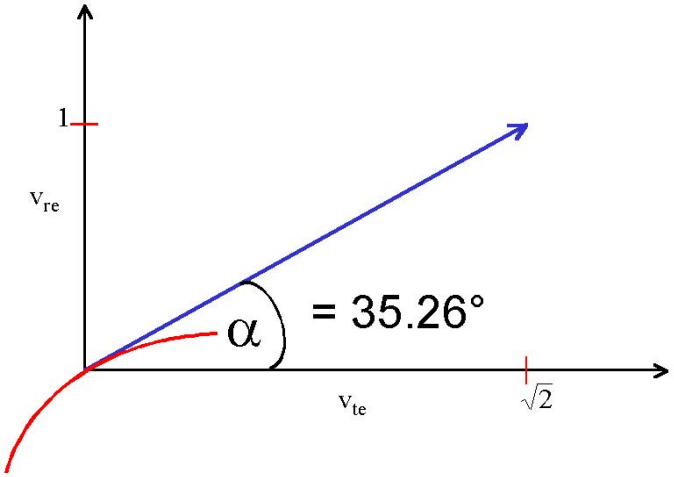

Fig. 5.11: Orthogonal vectors with ratio $1/\sqrt{2}$ = 0.7071; arctan 0.7071 = 35.26°

An explanation for the fixed ratio of $1/\sqrt{2}$ can be given by calculating the local velocity at a given point on the disk electrode. The velocities in the tangential and the radial direction in the solution must therefore be described. Furthermore, in order to understand the pattern formation on the disk electrode, it is necessary to take into account the Coriolis force.
An expression for the velocity (v_t) in the tangential direction is given by the well known equation:

$$v_t = \omega \cdot r \tag{5.3}$$

Eq. 5.3: Tangential velocity (v_t); with: angular velocity (ω) and radius (r)

The radial velocity (v_r) component can be derived from the centrifugal acceleration:

$$a_{cf} = \omega^2 \cdot r \tag{5.4}$$

Eq. 5.4: centrifugal acceleration (a_{cf}); with: angular velocity (ω) and radius (r)

For constant acceleration (a_{cf}), an expression for the radial velocity can be derived in the classical manner:

$$t = \frac{v_r}{a_{cf}} \tag{5.5}$$

and:

$$r = \frac{1}{2} \cdot a_{cf} t^2 \tag{5.6}$$

Putting Eq. 5.5 into Eq. 5.6 results in an expression for dependence of velocity (v_r) on acceleration (a_{cf}) and distance (r):

$$v_r = \sqrt{2 \cdot a_{cf} \cdot r} = \sqrt{2 \cdot \omega^2 r^2} \tag{5.7}$$

Using Eq. 5.3, the radial velocity can now be specified:

$$v_r = \sqrt{2} \cdot \omega \cdot r = \sqrt{2} \cdot v_t \tag{5.8}$$

Eq. 5.8: Radial velocity (v_r); with: angle velocity (ω) and radius (r)

This simple integration of the centrifugal acceleration is only permissible if it can be presumed to be a constant acceleration. This is indeed the case, due to the formation of convection vortices in the boundary layer beneath the electrode (Fig. 5.12). On the one hand, every finite volume element of the solution has contact with the electrode surface for only an infinitesimal amount of time. On the other hand, there is no flux along the spirally shaped valleys in the electrode surface, since there is no mass exchange between neighboured vortex cells, which might be of 'horseshoe'-like character (Reed & Saric [1989]). Acceleration is therefore a very local phenomenon.

Fig. 5.12: Schematic representation of convection vortices (orange arrows) on an experimentally structured surface (blue)

For these areas, the vector sum (v*) of the radial (v_r) and tangential velocities (v_t) is the direction of the resultant flow in the vortices within the framework of the solution.

To describe the formation of patterns on the electrode surface, the frame of reference must be changed and the Coriolis force (F_C) taken into account.

$$F_c = 2m \cdot v^* \times \omega \tag{5.9}$$

Eq. 5.9: Coriolis force (F_C); with mass (m), resultant flow velocity in the solution (v*) and angular velocity (ω).

Because of the fixed ratio (v_r/v_t) of $\sqrt{2}$ in the solution and the vector product in the equation for the Coriolis force (Eq. 5.9), the Coriolis force always acts in a direction of 35.26° = arctan($1/\sqrt{2}$) (see Fig. 5.13).

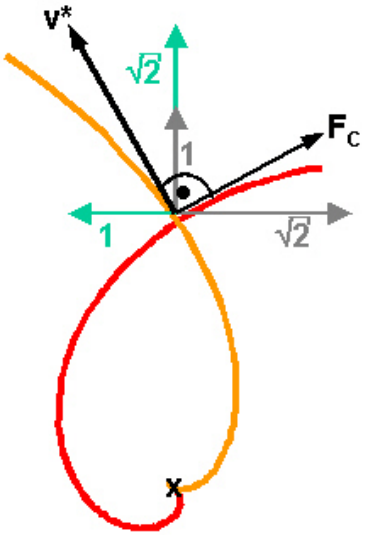

Fig. 5.13: v* and the orange line represent the flow direction in the vortices, in the non rotating framework (green coordinates); the Coriolis force (F_C) and the red line represent the flow in the framework of the rotating disk electrode (grey coordinates); **x** represents origin

This explains why logarithmic spirals with an overall angle of 35.26°, relative to the tangential direction, arise in rotating disk systems and why they are invariant in relation to the radius and very different rotational speeds.

5.5 Conclusion

Hydrodynamic pattern formation occurs on fast rotating disk electrodes under dissolution conditions. Instabilities of the laminar flow in the boundary layer can be expected, leading to the formation of swirling flows, composed of a sequence of convection vortices, forming logarithmic spirals. However, in contrast to the well known Görtler vortices, these spiral patterns do not turn in the boundary layer relative to the rotating disk. They are fixed to the disk surface due to the electrochemical process.

The dissolution of the electrode leads to surface roughness (subsection 5.3.1). This electrochemically produced roughness serves as an 'anchor' for the spirals and makes them rotate with the same angular velocity as the disk.
The spirals consist of a sequence of more or less isolated convection cells; small eddies with almost no convection flow between pairs of such convection cells. Small-volume elements of the electrolyte penetrate into these convection cells for a short time, undergoing an impulse in the direction v*, which is the overall vector sum of the tangential and radial velocity in this small region at the surface. The fresh incoming electrolyte leads to a stronger dissolution of the touched surface than the outgoing one, which is loaded with the ions of the dissolved metal of the electrode. This leads to the formation of spiral 'valleys' and 'walls' in the surface, respectively.
However, these spirals are curved in the opposite direction than the flow in the solution, because each volume element in a convection cell, moving with the overall resulting velocity ($v^* = v_t + v_r$), is subject to the Coriolis force (F_C), which acts in a direction perpendicular to the velocity v* within the framework of the rotating disk.
Since the ratio of the radial and tangential velocity amounts to $v_r / v_t = \sqrt{2}$ in any vortex cell, the characteristic angle α of the logarithmic spirals ($r = a \cdot e^{-(\tan\alpha)\cdot\Phi}$) results in $\alpha = \arctan(1/\sqrt{2}) = 35.26°$.
It is the local character of the electrochemically induced vortex cells in the spiral swirling flow that makes the ratio $1/\sqrt{2}$ an invariant of this pattern formation with respect to the Coriolis force within the framework of the rotating disk.

5.6 Acknowledgement

We are very grateful to the 'Deutsche Forschungsgemeinschaft' for financial support (PL 99/8-1 and PL 99/8-2). We also thank Prof. A. Visser (Fertigungstechnik, Universität Bremen) for his constant willingness for discussing our results and providing the microfocus scanner (UBM). In addition, we are indebted to Prof. R. Friedrich and his workgroup (Institute for Theoretical Physics, Universität Münster) for some inspiring discussions.

5.7 References

BASF Info Service [2001] "Viskosität von Eisen(III)Chlorid Lösung", internet info service.

Baune, M. & Plath, P.J. [2002] "Chemically Induced Hydrodynamic Pattern Formation: Slowly Rotating Disk Electrode under Dissolving Conditions and Genesis of Spatial Bifurcation", *Int. J. Bifurcation and Chaos* **12**(10), in press.

Bassett, M.R. & Hudson, J.L. [1990] "The Oscillatory Electrodissolution of Copper in Acidic Chloride Solution", *J. Electrochem. Soc.* **137**, 1815-1826.

Cochran, W.G. [1934] "The flow due to a rotating disc", *Cambridge Philosophical Society Proceedings* **30**, 365-375.

Fette, U. [1995] *Galvanostatische Potentialoszillationen und elektrochemisches Auflösungsverhalten von Edelstahl in Eisen(III)-chloridlösung, Ein neues oszillierendes System* (PhD Thesis, Universität Bremen) Chap. 7, pp. 27-30.

Gregory, N., Stuart, J.T. & Walker W.S. [1955] "On the Stability of Three-Dimensional Boundary Layers with Application to the Flow due to a Rotating Disk", *Mathem. and Phys. Sciences* **248**, 155-199.

Kármán, Th.v. [1921] "Über laminare und turbolente Reibung", *Zeitschrift für Angewandte Mathematik und Mechanik* **1**, 233-252.

Kobayashi, R., Kohama, Y. & Takamadate, Ch. [1980] "Spiral Vortices in Boundary Layer Transition Regime on a Rotating Disk", *Acta Mechanica* **35**, 71-82.

Kuiken, H.K. & Tijburg, R.P. [1999] "Centrifugal Etching: A Promising New Tool to Achieve Deep Etching Results", *The Journal PCMI* **May**, 10-20.

Leneweit, G., Roesner, K.G. & Koehler, R. [1999] "Surface instabilities of thin liquid film flow on rotating disk", *Experiments in Fluids* **26**, 75-85.

Levich, V.G., [1962] *Physicochemical Hydrodynamics* (Prentice-Hall, Inc., Englewood Cliffs, N.J.) pp. 66-67.

Piontelli, R., Rivolta, B. & Razzini G.C. [1969] "Esempi tipici di effetti morfologici del moto relativo solido-liquido nei processi elettrochimici", *Elektrochim. Metal*. **IV.3**, 218-233.

Reed, H.L. & Saric, W.S. [1989] "Stability of Three-Dimensional Boundary Layers", *Ann. Rev. Fluid Mech.* **21**, 235-284.

Riddiford, A.C. [1966] "The Rotating Disk System", *Advances in Electrochemistry and Electrochemical Engineering* **4**, 47-116.

Roger, G.T. & Taylor, K.J. [1963] "Effect of small Protrusions on Mass Transport to a Rotating-Disk Electrode", *Nature* **200**, 1062-1064.

Roger, G.T. & Taylor, K.J. [1975] "The Electrodeposition of Copper from Alkaline Cyanide Solution-II", *Electrochimica Acta* **20**, 703-707.

Visser A. & Buhlert M. [1999] "Theoretical and Practical Aspects of Fine Line Etching of Alloy 42", *The Journal PCMI* **May**, 21-26.

Yee, K.E. & Jorne, J. [1990] "Striated Zinc Electrodeposition at Rotating Disk and Hemisphere Electrodes", *J. Electrochem. Soc.* **137**(8), 2403-2410.

6 Galvanostatic Potential Oscillations in a System with Electrochemically Induced Hydrodynamic Pattern Formation: Two Different Phenomena*

Abstract

An electrochemical system of technical relevance - stainless steel in a highly concentrated iron(III) chloride solution - exhibiting permanent galvonostatic potential oscillation was studied. The system was chosen as a typical example for a metal that cannot be passivated under such conditions. The experiments were carried out on a rotating disk electrode under dissolving conditions. Differing oscillations were found in addition to pure electrochemical oscillations, as are well known, for example, from the system comprising iron in H_2SO_4 solution. These new, additional oscillations are caused by spatial patterns of the rotating disk electrode. However, the patterns are generated by coupling between the hydrodynamic pattern formation beneath the electrode and the strong electrochemical dissolution process.

6.1 Introduction

During anodic dissolution of iron in a highly concentrated iron(III) chloride solution, oscillatory behaviour was observed that resembles many other examples for metals in aqueous solutions.[1-5] As far back as the early 19th century, G.Th. Fechner[6] described electrochemical oscillations for the system comprising iron/silver in HNO_3 solution. In 1900, W. Ostwald[7,8] reported in detail about periodic phenomena during dissolution of chromium in acid solution. Many experimental and theoretical studies of the oscillatory behaviour of metals in various aqueous solutions can be found in the literature to date.[9-16]
An electrochemical model for current oscillations under potentiostatic conditions was first described by Franck & FitzHugh[17]. Not only were current oscillations in electrochemical systems observed, but also periodic potential oscillations under galvanostatic conditions - the focus of interest in our own experiments. These potential oscillations have been

* This chapter is based on the article: *"Galvanostatic Potential Oscillations in a System with Electrochemically Induced Hydrodynamic Pattern Formation: Two Different Phenomena."* (M. BAUNE and P. J. PLATH, Submitted to PCCP).

attributed to the formation of an unstable porous precipitation on the surface of the metal electrode, as opposed to the formation of a very dense passivating oxide layer.[18,19]
In addition to the aforementioned current and potential oscillations during anodic dissolution of metals in various aqueous solutions, the formation of topographical patterns in the surface of rotating disk electrodes under dissolving conditions has also been reported.[19-25] The question thus arises as to whether there is an interaction between rotation, electrochemical processes and pattern formation, on the one hand, and oscillatory behaviour, on the other.
In this paper, we describe the results of an investigation into galvanostatic potential oscillations during electro-dissolution of iron in highly concentrated iron(III) chloride solution with rotating disk electrodes. Different regimes with stationary, oscillatory or chaotic character were identified. By analysing the oscillatory behaviour in detail, a pure electrochemical signal could be separated from a new oscillating signal. This oscillating potential signal occurs during rotation of the working electrode, the surface of which has been structured by the coupling of electrochemical and hydrodynamic processes. Finally, it was possible to correlate the periodic potential-time signal with the topographical patterns formed in the surface of the electrode during dissolution.

6.2 Experimental Details

Experiments were carried out with a chromium-nickel steel disk electrode with a diameter of 5.0 mm, covered by a Teflon-jacket to protect the side walls of the cylinder. A platinum ring was used as counter electrode, which was placed in the same plane as the working disk electrode to obtain a symmetrical distribution of current density in the solution. The Ag/AgCl reference electrode was positioned via a capillary adjacent to the perimeter of the working electrode to minimise the influence on the hydrodynamics beneath the rotating electrode. A schematic diagram of the three-electrode setup is shown in Fig. 6.1.

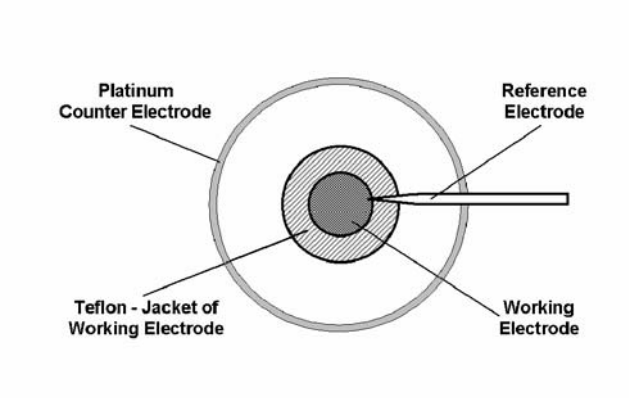

Fig. 6.1: Schematic diagram of the three-electrode setup which was used to perform the experiments

The current and the potential were controlled and measured using a Jaissle Potentiostat - Galvanostat (IMP 83 PC-2), which enabled potentiodynamic as well as galvanodynamic experiments to be carried out. Data was recorded directly (20 Hz, 12 bit) on a personal computer. The rotational speed could be adjusted and controlled in a range between 1 and 6000 revolutions per minute (rpm) by means of a Jaissle R.S. PI control unit.
All experiments were carried out in a highly concentrated iron(III) chloride solution (3.5 M).
To observe the pattern formation on the electrode as well as the hydrodynamic flow in the solution during all the experiments, a specially developed lightning source was used, and single pictures were taken by a CCD-camera and recorded by a personal computer. More details of the setup have been described previously.[20,21]
The exact topography of the complete electrode surface with a diameter of 5 mm was measured with a resolution of 5 μm by a LASER focus scanner (UBM microfocus).

6.3 Results

A typical current-potential curve of the system comprising a steel disk electrode in concentrated iron(III) chloride solution, without rotation, is shown in Fig. 6.2. The forth-scan (lower curve) follows a step-like behaviour before it reaches a limited current plateau, whereas the back scan (upper curve) does not exhibit this step-like behaviour. The sweep rate was 2 mV/s. For comparison purposes, see also Fette and Plath[19], where, with a different setup, the step-like behaviour could be found for the first forth-scan only. Additional experiments have proven that the disappearance of the step-like behaviour for the second and following forth-scans is caused by the reference electrode. By using a circular frit of the same diameter as the working electrode and placed exactly beneath the disk, instead of a capillary as reference electrode, the step-like behaviour can be found for the first forth-scan only.

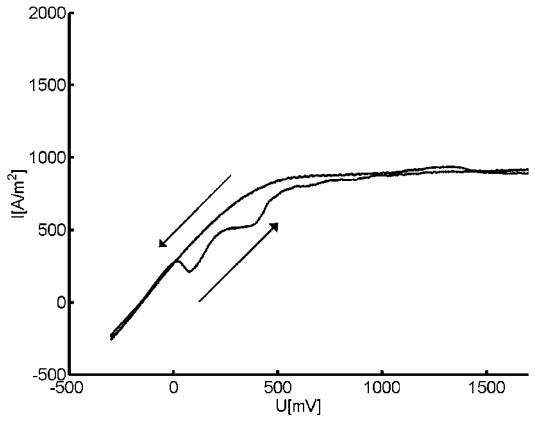

Fig. 6.2: Back and forth scan of a non rotating disk electrode in 3.5 M iron(III) chloride solution using a sweep rate of 2 mV/s

The step-like behaviour of the potentiodynamic scan, including regions with negative slope, and the onset of potential oscillations indicate the formation of precipitate on the surface of the metal electrode as it is detailed by Li et al.[5] (see also Ref.[19,25]). These precipitate layers are influenced by the rotational speed.

Standard voltammograms were generated in order to characterise the system under consideration and to observe the dependency of current behaviour on the rotational speed of the working electrode (Fig. 6.3).

The step-like behaviour of the poteniodynamic scan is found to disappear with increasing rotational speed, and could only be found at rotational speeds lower than about 50 rpm. Furthermore, the overall behaviour of the current increasingly obeys Ohm's law at higher rotational speeds. The dependence of the dissolution current on the rotational speed indicates that the current is limited by transport.

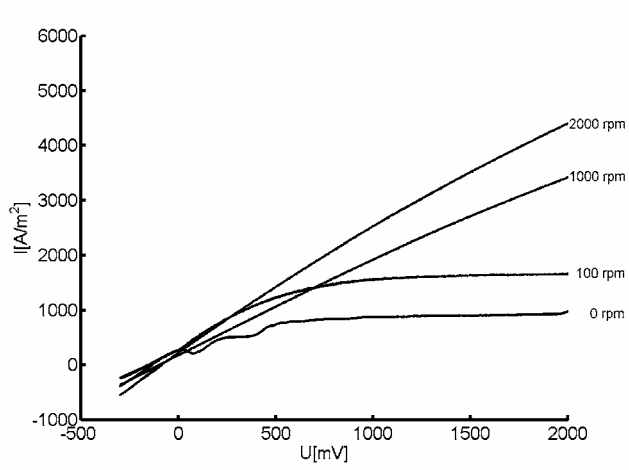

Fig. 6.3: Voltammogram at different rotational speeds

All these potentiodynamic experiments form the framework and basis for the parameters (current density and rotational speed) to be chosen in order to find oscillatory behaviour under galvanostatic conditions.

It is difficult to decide, on the basis of the galvanogram (Fig. 6.4), in which region or regions of current density oscillations are likely to occur. In Fig. 6.4, the curve is plotted in the same way as in the voltammograms shown above (Figs. 6.2 and 6.3), but in this graph the scanned parameter was current density (y-axis). Nevertheless, for four regions of current density the possibility of non-trivial behaviour is suggested (see also Fette & Plath[19]).

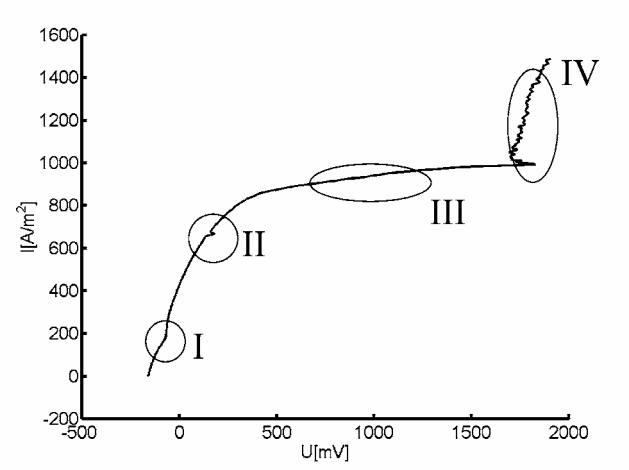

Fig. 6.4: Galvanogram with a sweep rate of 0.5 A/m^{2}s; there are four distinctive regions in which oscillations could occur

The behaviour in the different regions over time was examined by slowly scanning to each of them and holding current density constant at that point for half an hour. Only regions I and II show steady-state behaviour. For this reason, only the result for region I (lower curve) is plotted as an example in Fig. 6.5. This again contrasts with Fette and Plath[19], but is also caused by the different setup as mentioned before. In region III (grey curve, Fig. 6.5), an oscillatory state with high amplitude and low frequency was observed, whereas the temporal behaviour in region IV (black curve, Fig. 6.5) shows chaotic behaviour with a lower amplitude than the oscillations in region III.

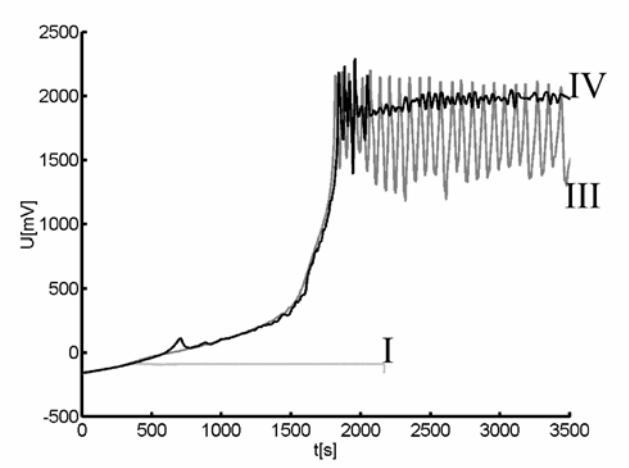

Fig. 6.5: Time series over 30 min after scanning to the regions I, III and IV

In order to visualise the oscillatory and the chaotic behaviour more clearly, the delay plots of these time series (III and IV from Fig. 6.5) are shown in Fig. 6.6.
The plot on the left represents the almost periodic behaviour of region III, whereas the plot from region IV, on the right, does not follow such a simple path through the phase space.

To characterise this chaotic behaviour exactly it is necessary to perform further mathematical analysis, but this was not the subject of research in the present work.

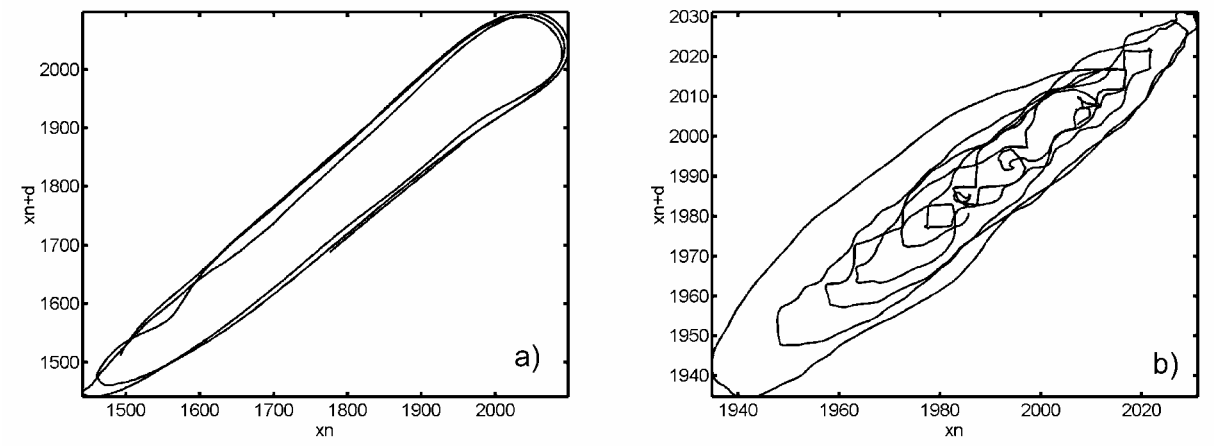

Fig. 6.6: Phase space diagrams of the time series; a) region III and b) region IV

Stationary, oscillatory and chaotic behaviour was found for the system comprising a steel disk electrode in concentrated iron(III) chloride solution, without rotation of the disk electrode.[25] Investigations were therefore focused on the influence of rotation and pattern formation on the galvanostatic time behaviour.

Rotation was firstly added to the system in the steady-state region (see region I and II in Figs. 6.4 and 6.5).

A rotational speed of 10 rpm was applied to the system. The mean potential in this experiment remained the same as the potential that the system reaches without rotation. However, the time behaviour is now superposed by periodic oscillations. This oscillatory behaviour is completely different, in terms of amplitude and frequency, to the oscillations found in region III (see Fig. 6.5). Figure 6.7 shows a segment of the behaviour of the potential over time for a rotational speed of 10 rpm (left graph; Fig. 6.7a). In the right-hand graph (Fig. 6.7b) the corresponding Fourier spectrum is shown and Fig. 6.7c depicts the topographical structure of the surface appendent to the time series and the Fourier spectrum (Fig. 6.7a&b).

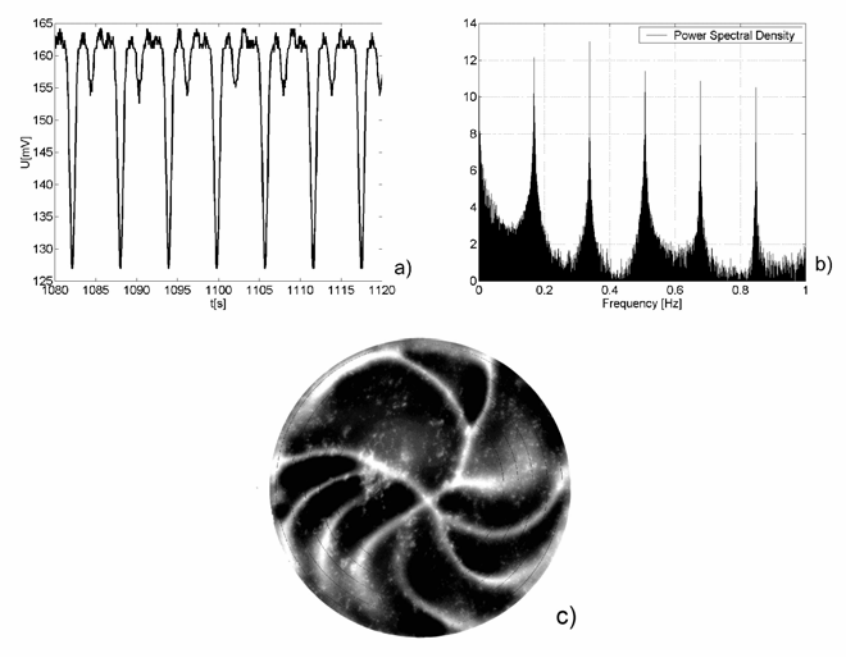

Fig. 6.7: a) Segment of time behaviour of potential at 10 rpm and I = 668 A/m^2, b) Corresponding Fourier spectrum and c) Topography of the surface

The Fourier spectrum displays the main frequency of 0.17 Hz of the potential time behaviour. The rotational speed of 10 rpm is exactly equivalent to the same frequency of 0.17 Hz . This result shows that the oscillatory behaviour of the measured potential is correlated to the rotation of the disk electrode.
Additional periodic behaviour also occurs in the electrochemical oscillatory regime (region III; Fig. 6.4) with the onset of rotation. As can be seen from the two time series in Fig. 6.8, the main, low frequency does not change, with only the amplitude being lower in the case of additional rotation (black curve; Fig. 6.8). The grey curve (Fig. 6.8) is a segment of the time series of the electrochemical oscillation of the non-rotating electrode, as already shown in Fig. 6.5 (region III). The decrease of amplitude could be explained by the change of the diffusion boundary layer due to the onset of hydrodynamic flow, whereas the superimposed small oscillations are caused by the topographical structure formed in the electrode surface.

Fourier analysis of the time series with rotation of 10 rpm shows clearly that the small periodic fluctuations of the black curve again reflect the rotational movement of the disk electrode.

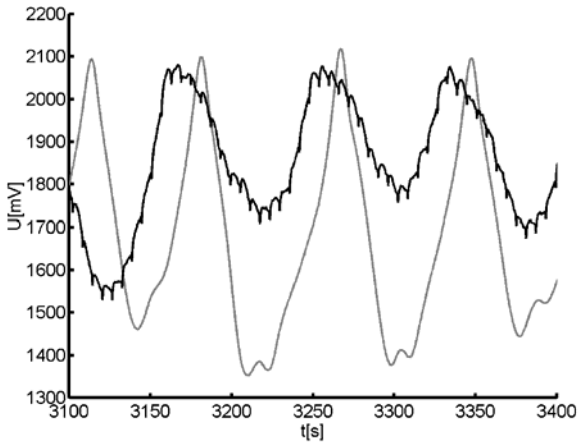

Fig. 6.8: Time series in the electrochemical oscillatory regime (III); grey curve: without rotation; black curve: with rotation of 10 rpm; both at 900 A/m^2

With the onset of rotation in the electrochemical system, not only does the time behaviour of the potential under galvanostatic conditions change - the surface of the disk electrode also becomes structured in the range of about 20 to 50 micrometers in depth and some hundred micrometers in width. The pattern formation is determined by hydrodynamic vortices in the boundary layer beneath the rotating disk electrode, which we reported on previously in some detail.[20,21]

As an example, Fig. 6.9 images an electrode surface after an experiment at 18 rpm and current density of 668 A/m^2. The darker parts have been etched deeper into the metal surface of the disk electrode. The reference electrode was placed at the edge of the electrode. Here the white line indicates the path followed by the reference electrode during rotation of the disk electrode.

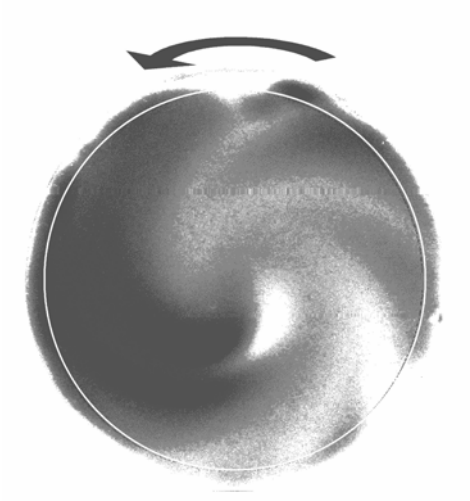

Fig. 6.9: LASER-scan image of an electrode surface after an experiment with rotation at 18 rpm and a current density of 668 A/m^2; the white line indicates the position of the reference electrode

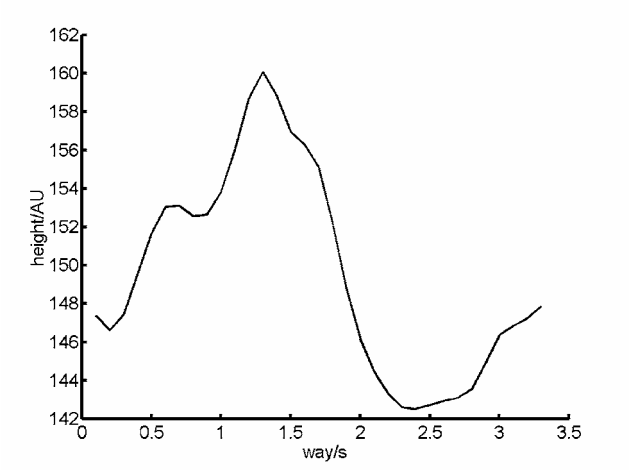

Fig. 6.10: Circular height profile of electrode surface at the reference electrode position. (The value of 'height/AU' means μm but with an arbitrary origin.)

From the electrode surface data (see Fig. 6.9), a circular height profile at the position of the reference electrode, indicated by the white line in Fig. 6.9, was extracted. This profile is shown in Fig. 6.10. On the x-axis the path traced by the electrode at 18 rpm is imaged as a function of the time that the electrode needs for one full revolution.

To investigate how the profile of the electrode surface influences the oscillations that occur when the electrode is rotating, the profile shown in Fig. 6.10 was correlated with the time signal for the potential in the corresponding experiment. Although the time behaviour of the potential (upper graph of Fig. 6.11) changes slightly, the correlation function (lower graph of Fig. 6.11) has almost a sinusoidal shape.
This means, with every full revolution, the surface and the time behaviour of potential is almost completely correlated.

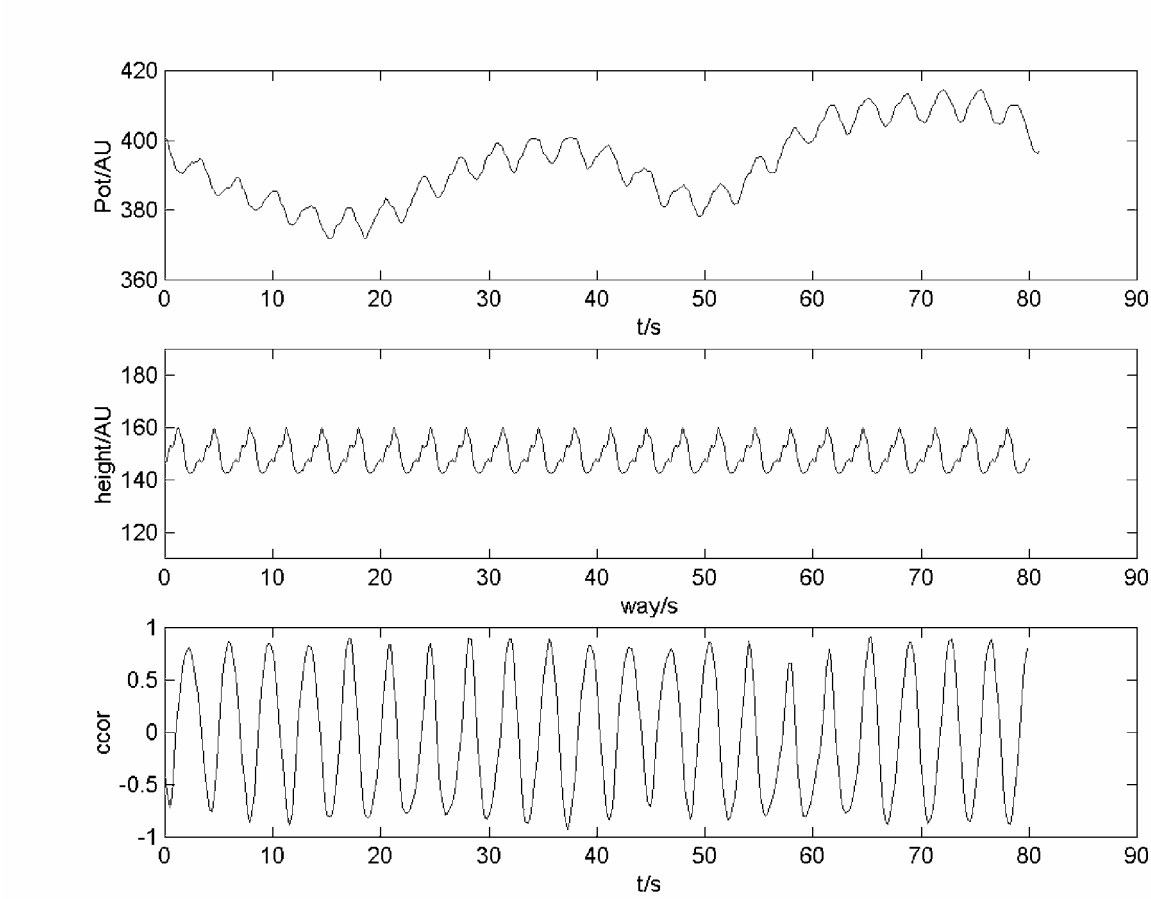

Fig. 6.11: Correlation function (lower graph) of the time behaviour of potential (upper graph) and the radial height profile of the electrode surface (middle graph; showing the height profile for all full revolutions of the time series, for better visualisation)

6.4 Concluding remarks

The dynamics of the system - stainless steel in highly concentrated iron(III) chloride solution - were investigated. The materials used are relevant for common technological processes.[26-29] The working steel electrode consists of a chromium nickel alloy with a statistically homogeneous distribution of the different metals of the alloy, but local variations of the chemical composition. The solution used, unusual for electrochemical research studies, is highly concentrated, very acidic, oxidising and contains chloride. As under scientifically idealised conditions, also for the non-ideal system, different regions of stationary state, oscillatory and chaotic behaviour could be found and generated reproduceable. Purely on account of the non-ideal conditions, additional phenomena for electrochemical system were found. An oscillatory behaviour caused by the rotating topographically structured electrode and different from typical electrochemical oscillation was identified. It was shown that these oscillations occur only during rotation of the

working electrode. Furthermore, it was demonstrated that the oscillating behaviour of the time series of potential is directly influenced by the topography of the surface of the working electrode. This was characterised by the cross-correlation function between the time signal and a circular height profile of the structured surface.
Additional proof can be provided for the direct correlation between the topography of the structured surface and the oscillatory time behaviour at the rotating disk electrode. At the beginning of each experiment, a new, unstructured electrode was used. Therefore, no oscillations, caused by the topographically structured surface, should occur at the beginning of the experiments, as illustrated in Fig. 6.12. To avoid overshooting of the potential, the current was increased slowly up to a fixed value of potential density. During this time, the spatial pattern develops in the electrode surface. Associated with the formation of this spatially structured surface, the amplitude of the potential oscillations also rises. Because of this, an onset of the oscillations by a badly bedded electrode can also be excluded.

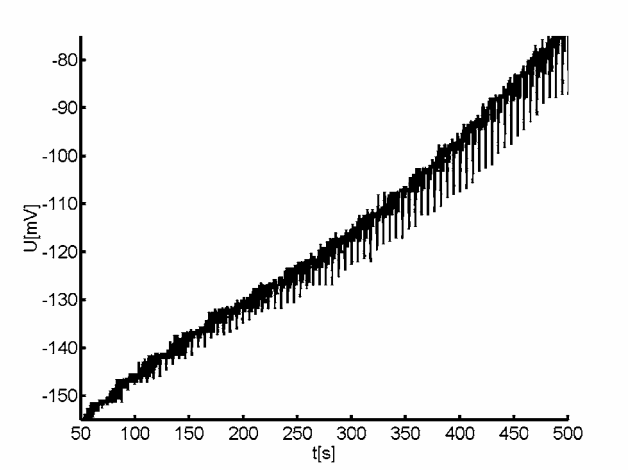

Fig. 6.12: Development of the potential oscillations at the formation of structured patterns on the electrode, in the beginning of an experiment (0 - 200 A/m^2 and a constant rotational speed of 10 rpm)

Feedback exerted by the reference electrode on the current control can also be excluded as a reason for potential oscillations. In the galvanostatic operational range of the Jaissle Potentiostat - Galvanostat (IMP 83 PC-2), the reference electrode is only used for potential monitoring at the working electrode and has no influence on the regulation of current.
Recapitulating, it should be pointed out that a new type of potential oscillation in time series occurs at a rotating disk electrode under dissolving conditions. These oscillations can be explicitly correlated with the circular height profile of the spatial pattern developing in the surface of the slowly rotating and dissolving disk electrode.
This new type of superimposed oscillation is caused by the interference of chemically induced hydrodynamic vortex patterns in the boundary layer beneath the rotating electrode and the oscillating electrochemical dissolution process. Both these instabilities are coupled via the topographical structuring of spiral patterns in the electrode surface.

This oscillating system may be important for technological systems, because precisely such non-ideal technical conditions can exhibit even richer dynamic behaviour than idealised scientific systems. The investigation of pattern formation and the correlation between the surface structure and potential oscillations at the slowly rotating disk electrode could open up new approaches to technological problems in the field of galvano-techniques (metal dissolution and deposition) and surface structuring. Just because of the slow rotational speed of the working electrode it can be compared with slowly moved workpieces though a reactive solution or the slow flow of solution along the workpiece. In all these technical processes a coupling beween the hydrodynamics and the electrochemical reaction can lead to unforeseen manufacturing errors.

6.5 Acknowledgement

We are very grateful to the 'Deutsche Forschungsgemeinschaft' for financial support (PL 99/8-1 and PL 99/8-2). We also thank Prof. A. Visser (Production Technology, University of Bremen) for his constant willingness to discuss our results and for providing the microfocus scanner (UBM). In addition, we are indebted to Prof. R. Friedrich and his workgroup (Institute for Theoretical Physics, University of Münster) for some inspiring discussions.

6.6 References

1 P. Russell and J. Newman, *J. Electrochem. Soc*., 1987, **133**(1), 1051-1058.
2 M. R. Bassett and J. L. Hudson, *J. Electrochem. Soc*., 1990, **137**(6), 1815-1826.
3 D. Sazou, A. Karantonis and M. Pagitsas, *Int. J. Bifurcation and Chaos*, 1993, **3**(4), 981-997.
4 J. F. Cooper, R. H. Muller and C. W. Tobias, *J. Electrochem. Soc*., 1980, **127**(8), 1733-1744
5 W. Li, K. Nobe and A. J. Pearlstein, *J. Electrochem. Soc*., 1993, **140**(3), 721-728.
6 G. Th. Fechner, *Schweigg. J. (Jahrb. d. Ch. u. Ph.)*, 1828, **53**, 129-151.
7 W. Ostwald*, Z. Phys. Chem*., 1900, **35**, 33-76.
8 W. Ostwald, *Z. Phys. Chem*., 1900, **35**, 204-256.
9 H.-H. Strehblow and J. Wenners, *Electrochim. Acta*, 1977, **22**, 421-427
10 J. L. Hudson and T. T. Tsotsis, *Chem. Eng. Science*, 1994, **49**(10) 1493-1572.
11 J. Woitowicz, in: *Modern Aspects of Electrochemistry*, ed B. E. Conway and J. O'M. Bockris, Butterworth , London, 1973, **8**, p. 47-120.
12 J. L. Hudson and M. R. Bassett, Rev. in: *Chem. Eng*.,1993, **7**(2) 109 - 169.

13 M. Baune, F. Ahrlich, U. Sydow and P. J. Plath, Prog. *Theor. Phys. Suppl*., 2000, **139**, 437-444.
14 L. Ma and J. E. Vitt, *J. Electrochem. Soc*., 1999, **146**(11), 4152-4157.
15 M. Eiswirth, A. Freund and J. Ross, *Adv. Chem. Phys*. 1991, **80**, 127
16 N. I. Jaeger, R. D. Otterstedt, A. Bîrzu, B. J. Green and J. L. Hudson, *Chaos*, 2002, **12**(1), 231-239.
17 U. F. Franck and R. FitzHugh, *Z. Elektrochem*., 1961, **65**(2), 156-168.
18 M. Z. Yang, J. L. Luo and M. Wilmott, J. Materials. *Sc. Lett*., 1998, **17**, 1071-1075.
19 U. Fette and P. J. Plath, *Z. Phys. Chem*., 1998, **205**, 143-165.
20 M. Baune and P. J. Plath, *Int. J. Bifurcation and Chaos*, 2002, **12**(10), in press.
21 M. Baune, V. Breunig-Lyriti and P. J. Plath (Accepted for: *Int. J. Bifurcation and Chaos*, 2002)
22 K. Krischer, in *Modern Aspects of Electrochemistry*, ed. B. E. Conway, J. O'M. Bockris and R. E. White, Kluwer Academic/Plenum, New York, 1999, **32**, p.1-142.
23 A. C. Riddiford, *Electrochemistry and Electrochemical Engineering*, 1966, **4**, 47-116.
24 G. T. Roger and K. J. Taylor, *Nature*, 1963, **200**, 1062-1064.
25 U. Fette, *PhD Thesis*, Universität Bremen, 1995.
26 A. Visser, *The Journal PCMI*, 1987, **30**, 8-15.
27 H. K. Kuiken and R. P. Tijburg, *The Journal PCMI*, 1999, **May**, 10-20.
28 M. Buhlert, , *PhD Thesis*, Universität Bremen, 2000.
29 A. Visser and M. Buhlert, *The Journal PCMI*, 1999, **May**, 21-26.

7 Summary

In the present work, experimental and theoretical results relating to the etching process at rotating steel disk electrodes in highly concentrated iron(III) chloride solution (3.5 M) are presented.

The onset of a natural convection flow caused by the strong dissolution process in the gravity field was shown for non- and slowly rotating stainless steel (1.4301) electrodes. Coupling between this natural flow, the dissolution of metal and the rotation of the electrode was visualised, and led to the conclusion that convection vortices are generated in the boundary layer beneath the electrode. Due to this effect, the pattern formation for non- and slow rotational speeds (0 - 50 rpm) could be explained in detail using a phenomenological model, which explains the onset of a main flow in the bulk solution, on the one hand, and the generation of convection vortices in the boundary layer, on the other. The occurrence of spatial bifurcations could also be described in terms of the formation of convection vortices.

A transition region that does not evidence a topographically structured surface was observed. This region signifies the point at which the two forces acting in opposite directions – gravitational and centrifugal force – are in balance.

At slow rotational speeds ($\omega < 15$ rpm), gravitational force dominates, resulting in a main convection flow from edge to centre directly beneath the electrode. In contrast, domination of the centrifugal force at higher rotational speeds ($\omega > 15$ rpm) changes the direction of main flow from the centre to the edge, which is the reason for the change of curvature direction in the patterns thus generated.

Based on these results, it was possible to show in detail the importance of gravitational force for the hydrodynamics of a dissolving and slowly moving electrode.

Compared to the different patterns formed at slow rotational speeds, careful study of the system using fast rotating electrodes (1000 - 6000 rpm) under different operating conditions (rotational speed, temperature, current density and geometrical boundary conditions) showed invariant pattern formation behaviour.

A simple physical model was elaborated that can describe the formation of the logarithmic spiral-shaped patterns. This result contrasts with the classical explanation of pattern formation at fast rotating disks. In many cases the latter is merely interpreted as an image of the hydrodynamic flow beneath the disk (Levich [1962]). However, the Coriolis force has to be taken into account in order to describe the whole process. With this basic approach, the invariant ratio of $1/\sqrt{2}$ of the flow field with respect to the rotation of the disk could be clarified.

This system with electrochemically induced hydrodynamic pattern formation also exhibits permanent galvanostatic potential oscillations, as known from many other examples for metals in aqueous solutions.
The interaction between electrochemical oscillations and topographical pattern formation due to dissolution and rotation was investigated. Different regimes of current density were identified, showing stationary, oscillatory and chaotic behaviour.
A superimposed oscillation, relative to the classical electrochemical oscillations, was identified, and correlated directly with the topography of the patterns generated in the surface of the rotating and dissolving electrode. The hydrodynamic vortex patterns in the boundary layer beneath the electrode and the electrochemical processes are coupled via the topographically structured surface and lead to this new type of superimposed potential oscillation.

The body of results obtained from these experiments provide a comprehensive analysis of moving workpieces in corrosive media, and of the coupling between electrochemical and hydrodynamic instabilities as exemplified in a system comprising rotating steel disk electrodes in highly concentrated iron(III) chloride solution.

8 References

Allen, D. M. [1986] *The Principles and Practice of Photochemical Machining and Photoetching* (Adam Hilger, Bristol and Boston).

Andersen, K. H., Abel, M., Krug, J., Ellegaard, C., Søndergaard, L. R. & Udesen, J. [2002] "Pattern Dynamics of Vortex Ripples in Sand: Nonlinear Modeling and Experimental Validation", *Physical Review Letters* **88**(23), 234302-1 - 234302-4.

Baier, G., Kummer, U. & Sahle, S. [1999] "An electrochemical induced oscillatory instability", *Journal of Physical Chemistry A* **103**, 33-37.

Balachandra, S., Street, C. L. & Malik, M. R. [1992] "Secondary instability in rotating-disk flow", *Journal of Fluid Mechanics* **244**, 323-347.

Balakumar, P. & Malik, M. R. [1990] "Traveling Disturbances in Rotating-Disk Flow", *Theoretical and Computational Fluid Dynamics* **2**, 125-137.

BASF Info Service [2001] "Viskosität von Eisen(III)Chlorid Lösung", internet info service.

Bassett, M. R. & Hudson, J. L. [1990] "The Oscillatory Electrodissolution of Copper in Acidic Chloride Solution", *Journal of The Electrochemical Society* **137**, 1815-1826.

Baune, M., Ahrlich, F., Sydow, U. & Plath, P. J. [2000] "The Intermittent Behaviour of a Platinum Electrode in Aqueous Solutions", *Progress of Theoretical Physics Supplement* **139**, 437-444.

Baune, M. & Plath, P. J. [2002] "Chemically Induced Hydrodynamic Pattern Formation: Slowly Rotating Disk Electrode under Dissolving Conditions and Genesis of Spatial Bifurcation", *International Journal of Bifurcation and Chaos* **12**(10), in press.

Baune, M., Breunig-Lyriti, V. & Plath, P. J. [2002] "Invariant Hydrodynamic Pattern Formation: Fast Rotating Disk Electrode Under Dissolving Conditions", accepted for *International Journal of Bifurcation and Chaos.*

Baune, M. & Plath, P. J. [submitted] "Galvanostatic Potential Oscillations in a System with Electrochemically Induced Hydrodynamic Pattern Formation: Two Different Phenomena", Submitted to *Journal of Physical Chemistry and Chemical Physics (PCCP).*

Bîrzu, A., Green, B., Jaeger, N. J. & Hudson, J. L. [2001] "Spatiotemporal Patterns during Electrodissolution of a Metal Ring: Three-dimensional Simulation", *Journal of Electroanalytical Chemistry* **504**, 126-136.

Bockris, J. O'M., Despic, A. & Drazic, D. M. [1961] "The Electrode Kinetics of the Deposition and Dissolution of iron", *Electrochimica Acta* **4**, 325-361.

Bonhoeffer, K. F. [1948] "Über periodische chemische Reaktionen I", *Zeitschrift für Elektrochemie*, **51** (1), 24-29.

Buhlert, M. [2000] *Elektropolieren und Elektrostrukturieren von Edelstahl, Messing und Aluminium: Untersuchung des transpassiven Abtragprozesses einschliesslich unerwuenschter Nebeneffekte*, (PhD Thesis, Universität Bremen).

Chin, R. J. & Nobe, K. [1972] "Electrodissolution Kinetics of Iron in Chloride Solution, III. Acidic Solutions", *Journal of The Electrochemical Society* **119**, 1457-1461.

Cochran, W. G. [1934] "The flow due to a rotating disc", *Cambridge Philosophical Society Proceedings* **30**, 365-375.

Cooper, J. F., Muller, R. H. & Tobias, C. W. [1980] "Periodic Phenomenon during Anodic Dissolution of Copper at high Current Densities", *Journal of The Electrochemical Society*, **127**(8), 1733-1744.

Eiswirth, M., Freund, A. & Ross, J. [1991] "Mechanistic Classification of Chemical Oscillators and the Role of Species", *Advanced Chemical Physics* **80**, 127-199.

Fechner, G. Th. [1828] "Zur Elektrochemie. 1. Ueber Umkehrungen der Polarität in der einfachen Kette", *Schweigger's Journal (Journal für Chemie und Physik)* **53**, 129-151.

Fette, U. [1995] *Galvanostatische Potentialoszillationen und elektrochemisches Auflösungsverhalten von Edelstahl in Eisen(III)-chloridlösung, Ein neues oszillierendes System* (PhD Thesis, Universität Bremen).

Fette, U. & Plath, P. J. [1998] "Galvanostatische Potentialoszillationen und anodisches Auflösungsverhalten von CrNi-Edelstahl in konzentrierter Fe(III)Cl_3-Lösung" *Zeitschrift für Physikalische Chemie* **205**, 143-165.

Flade, F. [1911] "Beiträge zur Kenntnis der Passivität", *Zeitschrift für Physikalische Chemie* **76**, 513-559.

Franck, U. F. & FitzHugh, R. [1961] "Periodische Elektrodenprozesse und ihre Beschreibung durch ein mathematisches Modell", *Zeitschrift für Elektrochemie*, **65**(2), 156-168.

Friedrich, R., Radons, G., Ditzinger, T. & Henning, A. [2000] "Ripple formation through a convective instability from moving growth and erosion sources", *Physical Review Letters* **85**(23), 4884-4887.

Gregory, N., Stuart, J. T. & Walker W. S. [1955] "On the Stability of Three-Dimensional Boundary Layers with Application to the Flow due to a Rotating Disk", *Mathematical and Physical Sciences* **248**, 155-199.

Günther, D. [2002] personal communication.

Hamann, C. H. & Vielstich, W. [1998] *Elektrochemie* (Weinheim; New York; Chichester; Brisbane; Singapore; Toronto: Wiley - VCH) pp. 237.

Hudson, J. L. & Bassett, M. R. [1993] "Oscillatory Electrodissolution of Metals", Review in *Chemical Engineering* **7**(2), 109-169.

Hudson, J. L. & Tsotsis, T. T. [1994] "Electrochemical Reaction Dynamics: A Review", *Chemical Engineering Science* **49**(10), 1493-1572.

Jaeger, N. I., Otterstedt, R. D., Bîrzu, A., Green, B. J. & Hudson, J. L. [2002] " Evolution of spatiotemporal patterns during the electrodissolution of metals: Experiments and simulation", *Chaos* **12**(1), 231-239.

Junker, M. [1994] *Hochdruck-/Hochtemperatur-Spruehaetzen von Wolfram, Molybdaen und Edelstahl* (PhD Thesis, Universität Bremen).

Kármán, Th.v. [1921] "Über laminare und turbolente Reibung," *Zeitschrift für Angewandte Mathematik und Mechanik* **1**, 233-252.

Kirchner, V., Cagnon, L., Schuster, R. & Ertl, G. [2001] "Electrochemical machining of stainless steel microelements with ultrashort voltage pulses", *Physical Review Letters* **79**, 1721-1723.

Kobayashi, R., Kohama, Y. & Takamadate, Ch. [1980] “Spiral Vortices in Boundary Layer Transition Regime on a Rotating Disk”, *Acta Mechanica* **35**, 71-82.

Kohama, Y. [1984] "Study on Boundary Layer Transition of a Rotating Disk," *Acta Mechanica* **50**, 193-199.

Krischer K. [1999] “Principles of Temporal and Spatial Pattern Formation in Electrochemical Systems”, *Modern Aspects of Electrochemistry* **32**, (Ed. By B.E. Conway *et al*. Kluwer Academic / Plenum Publishers, New York)

Kuiken, H. K. & Tijburg, R. P. [1999] "Centrifugal Etching: A Promising New Tool to Achieve Deep Etching Results", *The Journal of Photo Chemical Machining Institute* **73**, 10-20.

Kuo, H. C. & Nobe, K. [1978] "Electrodissolution Kinetics of Iron in Chloride Solutions, VI: Concentrated Acidic Solutions", *Journal of The Electrochemical Society* **125**(6), 854-860.

Lee, H. P., Nobe, K. & Pearlstein, A. J. [1985] " Film Formation and Current Oscillations in the Electrodissolution of Cu in Acidic Chloride Media", *Journal of The Electrochemical Society* **132**(5), 1031-1037.

Leneweit, G., Roesner, K. G. & Koehler, R. [1999] "Surface instabilities of thin liquid film flow on rotating disk", *Experiments in Fluids* **26**, 75-85.

Levich, V. G. [1962] *Physicochemical Hydrodynamics* (Prentice-Hall, Inc., Englewood Cliffs, N.J.) pp. 66-67.

Li, W., Wang, X. & Nobe, K. [1990] "Electrodissolution Kinetics of Iron in Chloride Solutions, VII: Experimental Potential/Current Oscillations", *Journal of The Electrochemical Society* **137**(4), 1184-1188.

Li, W., Nobe, K. & Pearlstein, A. J. [1993] "Electrodissolution Kinetics of Iron in Chloride Solutions, VIII: Chaos in Potential/Current Oscillations", *Journal of The Electrochemical Society* **140**(3), 721-728.

Li, W. & Nobe, K. [1993] "Electrodissolution Kinetics of Iron in Chloride Solutions, IX: Effect of Benzotriazole on Potential Oscillations", *Journal of The Electrochemical Society* **140**(6), 1642-1650.

Ma, L. & Vitt, J. E. [1999] " Current Oscillations during Iodide Oxidation at a Gold Rotating Disk Electrode", *Journal of The Electrochemical Society* **146**(11), 4152-4157.

McCafferty, E. & Hackermann, N. [1972] "Kinetics of Iron Corrosion in Concentrated Acidic Chloride Solutions", *Journal of The Electrochemical Society* **119**(8), 999-1009.

Newman, J. [1973] *Electrochemical Systems*, (Englewood Cliffs, New Jersey: Prentice Hall), pp. 280.

Ostwald, W. [1900, a] "Periodische Erscheinungen bei der Auflösung des Chroms in Säuren - Erste Mitteilung", *Zeitschrift für Physikalische Chemie* **35**, 33-76.

Ostwald, W. [1900, b] "Periodische Erscheinungen bei der Auflösung des Chroms in Säuren - Zweite Mitteilung ", *Zeitschrift für Physikalische Chemie* **35**, 204-256.

Otterstedt, R. [1997] *Raumzeitliche Strukturbildung bei der anodischen Auflösung von Kobalt in Phosphorsäure - Experimente und Modellierung* (PhD Thesis, Universität Bremen).

Pearlstein, A. J. & Johnson, J. A. [1989] "Global and Conditional Stability of the Steady and periodic Solutions of the Franck-FitzHugh Model of Electrodissolution of Fe in H_2SO_4", *Journal of The Electrochemical Society* **132**(9), 1290-1298.

Piontelli, R., Rivolta, B. & Razzini G. C. [1969] "Esempi tipici di effetti morfologici del moto relativo solido-liquido nei processi elettrochimici", *Electrochimica Metallurgia* **IV**(3), 218-233.

Press, F. & Siever, R. [1995] *Allgemeine Geologie* (Spektrum Akademischer Verlag Heidelberg; Berlin; Oxford) pp. 440.

Ramasawmy, H. & Blunt, L. [2002] "3D surface topography assessment of the effect of different electrolytes during electrochemical polishing of EDM surfaces", *International Journal of Machine Tools and Manufacture* **42**(5), 567-574.

Reed, H. L. & Saric, W. S. [1989] "Stability of Three-Dimensional Boundary Layers", *Annual Reviews of Fluid Mechanics* **21**, 235-284.

Riddiford, A. C. [1966] "The Rotating Disk System", *Advances in Electrochemistry and Electrochemical Engineering* **4**, 47-116.

Roger, G. T. & Taylor, K. J. [1963] "Effect of small Protrusions on Mass Transport to a Rotating-Disk Electrode", *Nature* **200**, 1062-1064.

Roger, G. T. & Taylor, K. J. [1975] "The Electrodeposition of Copper from Alkaline Cyanide Solution-II", *Electrochimica Acta* **20**, 703-707.

Russell, P. & Newman, J. [1987] "Anodic Dissolution of Iron in Acidic Sulfate Electrolytes II. Matematical Model of Current Oscillations observed under Potentiostatic Conditions", *Journal of The Electrochemical Society* **134**(5), 1051-1058.

Sazou, D., Karantonis, A. & Pagitsas, M. [1993] "Generalized Hopf, saddle-Node infinit period Bifurcations and excitability during the Electrodissolution and passivation of Iron in a sulfuric Acid solution" *International Journal of Bifurcation and Chaos* **3**(4), 981 - 997.

Schouveiler, L., Le Gal, P., Chauve, M. P. & Takeda, Y. [1999] "Spiral and circular waves in the flow between a rotating and a stationary disk", *Experiments in Fluids* **26**, 179-187.

Spohn, A., Mory, M. & Hopfinger, E. J. [1998] "Experiments on vortex breakdown in a confined flow generated by a rotating disc", *Journal of Fluid Mechanics* **370**, 73-99.

Strehblow, H.-H. & Wenners, J. [1977] "Investigation of the Process on Iron and Nickel Electrodes at high Corrosion Current Densities of high Chloride Content", *Electrochimica Acta* **22**, 421-427.

Sydow, U., Buhlert, M. & Plath, P. J. [accepted] "Characterization of Electropolished Metal Surfaces" accepted for: *Discrete Dynamics in Nature and Society*.

Visser, A. [1987] "Spray Etching of Stainless Steel - The Dependence of Stock Removal Rate on Alloying Elements and the Effects of High Sprayjet Pressures and High Etchant Temperatures", *The Journal of Photo Chemical Machining Institute* **30**, 8-15.

Visser A. & Buhlert M. [1996] "Elektrostrukturieren von Messingoberflächen, Untersuchung erwünschter und unerwünschter Abtrageffekte", *Galvanotechnik* **87**(5), 1454-1463.

Visser A. & Buhlert M. [1999] "Theoretical and Practical Aspects of Fine Line Etching of Alloy 42", *The Journal of Photo Chemical Machining Institute* **73**, 21-26.

Visser, A., Weissinger, D. & Ullmann, E. [1984]. "Werkstoffbearbeitung durch Sprühätzen", *Galvanotechnik* **75**(4), 414-424.

Wang, Y., Hudson, J. L. & Jaeger, N. I. [1990] "On the Franck-FitzHugh Model of the Dynamics of Iron Electrodissolution in Sulfuric Acid", *Journal of The Electrochemical Society* **137**(2), 485-488.

Woitowicz, J. [1973] *Oscillatory Behavior in Electrochemical Systems,* in: Modern Aspects of Electrochemistry, ed B. E. Conway and J. O'M. Bockris, Butterworth , London, **8**, p. 47-120.

Yang, M. Z., Luo, J. L. & Wilmott, M. [1998] "Oscillation of potential and current during the initiation of crevice corrosion on carbon steel", *Journal of Materials Science Letters* **17**(13), 1071-1075.

Yee, K. E. & Jorne, J. [1990] “Striated Zinc Electrodeposition at Rotating Disk and Hemisphere Electrodes”, *Journal of The Electrochemical Society* **137**(8), 2403-2410.

Abbreviations

CCD	Charge Coupled Device
LED	Light Emitting Diode
W	Watt
M	mol/dm³
mCd	milli Candela
pH	negative decade logarithm of proton concentration
rpm	revolutions per minute

List of figures

Appendix 1

Presentations of this work on national and international conferences and workshops

Talks:

25.-26. February 1999
Investigation of Nonlinear Dynamic Effects in Production Systems,
2nd International Symposium
Aachen Demonstration Laboratory for Integrated Production Engineering (ADITEC),
Aachen, Deutschland
Titel: *"Structure Formation during the Electrochemical Dissolution of Steel"*
U. Fette, V. Breunig-Lyriti, M. Baune, A. Visser & P. J. Plath

12.-19. March 2000
Grenzflächen, Turbulenz und Kritikalität,
14. Winterseminar auf dem Zeinisjoch / Tirol
Zeinisjoch, Österreich
Titel: *"Musterbildung bei der Auflösung von Stahl an der rotierenden Elektrode"*
M. Baune

09.-13. May 2000
Discrete Chaotic Dynamics in Nature and Society,
the second international conference (DCDNS2)
University of Southern Denmark, Odense University,
Odense, Dänemark
Titel: *"Pattern Formation During the Dissolution of Steel at the Rotating Disk Electrode"*
M. Baune

24.-26. May 2001
100. Hauptversammlung der Deutschen Bunsen-Gesellschaft
für Physikalische Chemie e.V.
Universität Stuttgart
Stuttgart, Deutschland
Titel: *"Experimental Studies of Pattern Formation at the Rotating Disk Electrode under Dissolving Conditions"*
M. Baune

07.-09. September 2001
European Science Foundation (ESF): REACTOR
Nonlinear Chemistry in Complex Reactors: Models and Experiments
University of Leeds,
Leeds, England, Großbritannien
Titel: *"Chemically Induced Hydrodynamic Pattern Formation"*
M. Baune

23. February - 02. March 2002
Multifraktales Skalenverhalten in Komplexen Systemen,
15. Winterseminar auf dem Zeinisjoch / Tirol
Zeinisjoch, Österreich
Titel: *"Spiralmuster bei der Auflösung von rotierenden Stahlelektroden"*
M. Baune

25. April 2002
Biophysik-Seminar,
Institut für Experimentelle Physik, Abteilung Biophysik
Otto-von-Guericke-Universität Magdeburg
Magdeburg, Deutschland
Titel: *"Chemically Induced Hydrodynamic Pattern Formation"*
M. Baune

Poster:

27. June - 11. July 1999
Let's Face Chaos Through Nonlinear Dynamics,
4th International Summer School/Conference
Universität Maribor, Slowenien
Titel: *"Investigation on the Complex Behaviour of a Platinum - Electrode in Aqueous Solutions"*
M. Baune, F. Ahrlich & P. J. Plath

20.-22. March 2000
System Science 2000, International Conference,
Integrative Approaches to Natural and Social Dynamics
Universität Osnabrück
Osnabrück, Deutschland
Titel: *"Pattern Formation during the Dissolution of Steel at the Rotating Disk Electrode"*
M. Baune, U. Fette, V. Breunig-Lyriti & P. J. Plath

01.-03. September 2000
Wilhelm Ostwald Symposium
Großboten, Deutschland
Titel: *"Pattern Formation during the Dissolution of Steel at the Rotating Disk Electrode"*
M. Baune, U. Fette, V. Breunig-Lyriti & P. J. Plath

26.-27. September 2000
Investigation of Nonlinear Dynamic Effects in Production Systems,
3rd International Symposium
Universität Cottbus
Cottbus, Deutschland
Titel: *"Pattern Formation during the Dissolution of Steel at the Rotating Disk Electrode"*
M. Baune, U. Fette, V. Breunig-Lyriti & P. J. Plath

Appendix 2

Chemicals & Materials

Iron(III)-chloride solution 40%

Specification
(by: Brenntag Chemiepartner)

Parameter	Unit	Method	Value
$FeCl_3$	w.-%	DIN 19602	40,0
Fe^{3+}	w.-%	DIN 19602	13,8
Cl^-	w.-%	DIN 19602	26,2
Density (20°C)	g/cm³	DIN 51757	1,42
pH-Value	pH		<1

Cr-Ni Stainless Steel

Specification
(by: Verlag Stahlschlüssel Wegst GmbH [1995])

Denotations	Composition	in %
	C	≤0,07
Cr-Ni Steel	Si	≤1,00
DIN 1.4301	Mn	≤2,00
X 5 CrNi 18 10	P	≤0,045
V2A	S	≤0,030
	Cr	17,0-19,0
	Ni	8,50-10,5
	Others	-

Danksagung

Ja, was soll ich sagen? Es gibt so viele, denen ich danken möchte. Der übliche Weg wäre natürlich der Einfachste. So etwas wie: "Ich danke meinem Betreuer Prof. Peter J. Plath für die Bereitstellung des Themas und für die zahlreichen Diskussionen."
Aber eigentlich würde ich viel lieber sagen, dass ich bei dir, Peter, gelernt habe, wie Wissenschaft 'funktioniert'.
"Auch danke ich Herrn Prof. Nils Jaeger für alle Anregungen und für die Begutachtung dieser Arbeit." Ich hoffe, dass sich Ihre anfänglichen Zweifel gegen die Art meiner Dissertation nicht bestätigt haben, und ich freue mich, dass Sie mir diese Möglichkeit gewährt haben.
Wem wird als nächstes gedankt? - In order of appearance? - Das geht ja nun wirklich nicht.
Meine Nummer eins: Claudia, in guten und in schlechten Tagen...
All meinen Freunden, für die unterschiedlichsten Dinge; alle namentlich zu nennen ist, glaube ich, nicht nötig, denn sie wissen das sie für mich da waren (und auch noch sind).
Karsten, Ute und Brigitte, die guten Seelen des Instituts, haben immer ein offenes Ohr und standen hilfreich zur Seite, und Kaffee war auch immer da.
"Ich danke der Arbeitsgruppe, deren Mitglied ich war, und allen im Institut für die gute Zusammenarbeit." Hendrik, du bist ein prima Raumteiler.
Da eine Promotion in der Regel nie ohne kleine (oder auch größere) technische Probleme vonstatten geht, kann ich mir auch meine Arbeit nicht ohne die wunderbare Unterstützung aller Mitarbeiter der universitären Werkstätten vorstellen.
Ein großes 'Dankeschön' geht auch nach Süddeutschland an Peter Schrems, vom Ingenieurbüro Peter Schrems, der bei allen Problemen und Fragen bezüglich des Potentiostaten, immer mit Rat und Tat zur Seite stand.
Allen Kolleginnen und Kollegen, die außerhalb der Bremer Universität zu finden sind, und die meine Irrwege durch die weite Welt gekreuzt haben, gilt mein Respekt, meine Anerkennung und natürlich auch mein Dank, denn oft habe ich durch ihre Kritik und Anregung erst den richtigen Weg gefunden. Hierbei möchte ich besonders die Arbeitsgruppen von Prof. Rudolf Friedrich (aus Stuttgart, jetzt Münster) und von Prof. Joachim Peinke (aus Oldenburg) hervorheben.
Von der DFG wurde ich durch die Projekte Pl 99/8-1 und Pl 99/8-2 finanziell unterstützt.
Falls ich jemanden vergessen haben sollte, dann geschah dieses ohne böse Absicht, und dieses 'Dankeschön' gilt all jenen.

No time we will make,
no time we will change,
but it's better to try,
than never to fly....

M.